# Fluorescence Detection of Ovarian Cancer in the NuTu-19 Epithelial Ovarian Cancer Animal Model using Aminolaevulinic Acid hexylester

Frank Lüdicke[1], Tanja Gabrecht[2], Norbert Lange[2], Georges Wagnières[2], Aldo Campana[1] and Attila Major[1]

[1]Department of Obstetrics and Gynecology, University Hospital, Geneva, Switzerland

[2]Institute of Environmental Engineering, Swiss Federal Institute of Technology (EPFL), Lausanne, Switzerland

In vivo fluorescence and light images of peritoneal tumor nodules. Fluorescence was excited using an endoscope (with D-light) after ip administration of ALA in an ovarian cancer rat (Fischer 344) model.

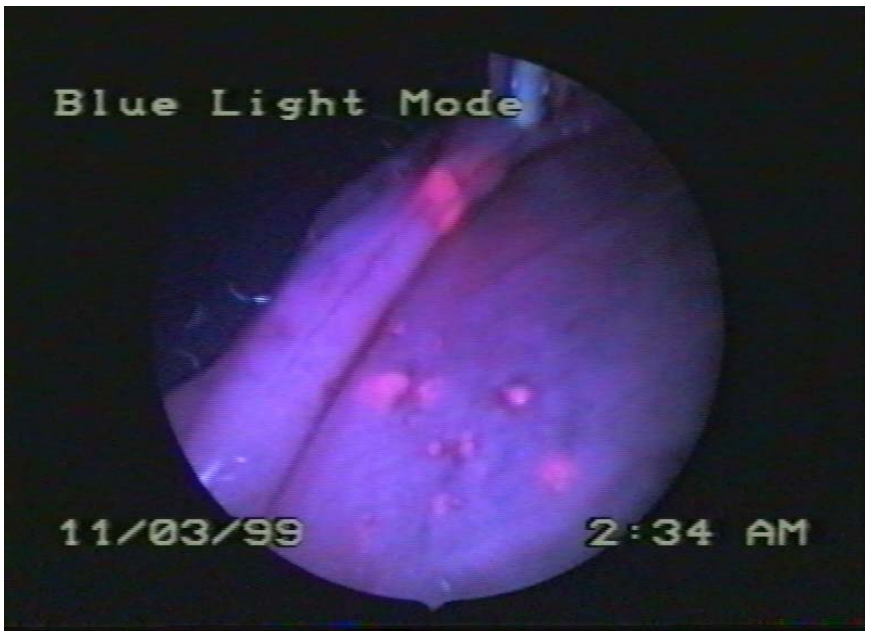


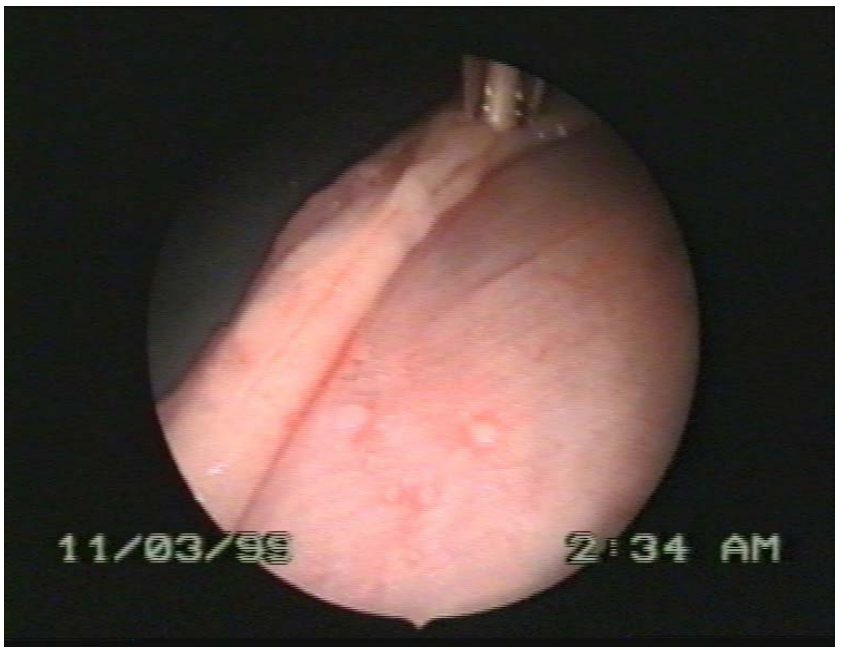

In vivo fluorescence and light images of peritoneal tumor nodules. Fluorescence was excited using an endoscope (with D-light) after ip administration of ALA in an ovarian cancer rat (Fischer 344) model.

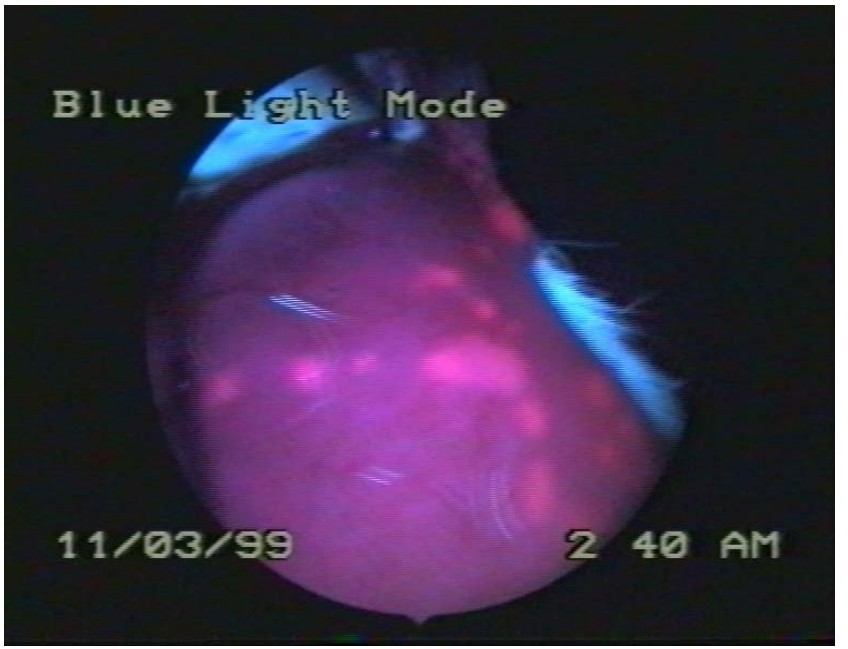


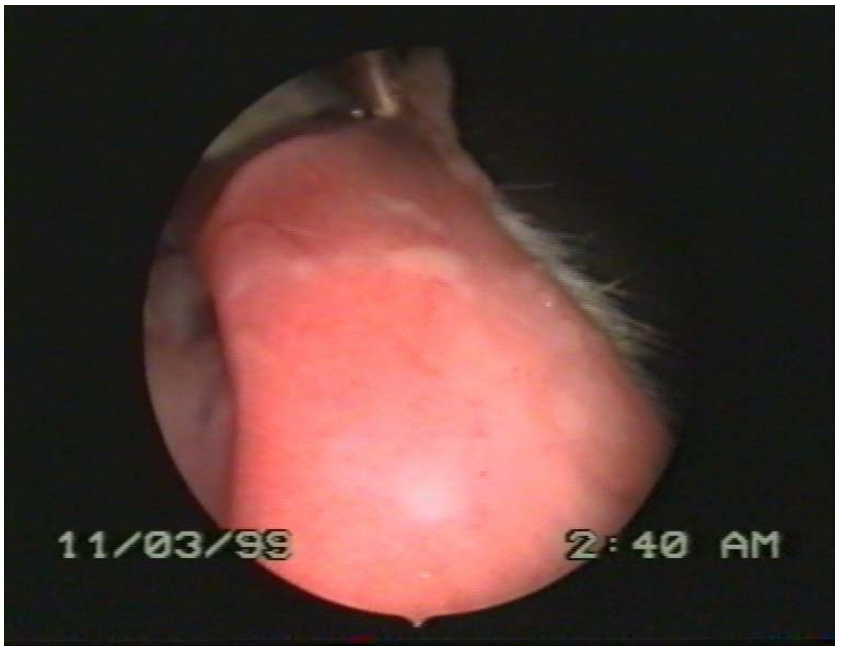

In vivo fluorescence and light images of peritoneal tumor nodules. Fluorescence was excited using an endoscope (with D-light) after ip administration of ALA in an ovarian cancer rat (Fischer 344) model.

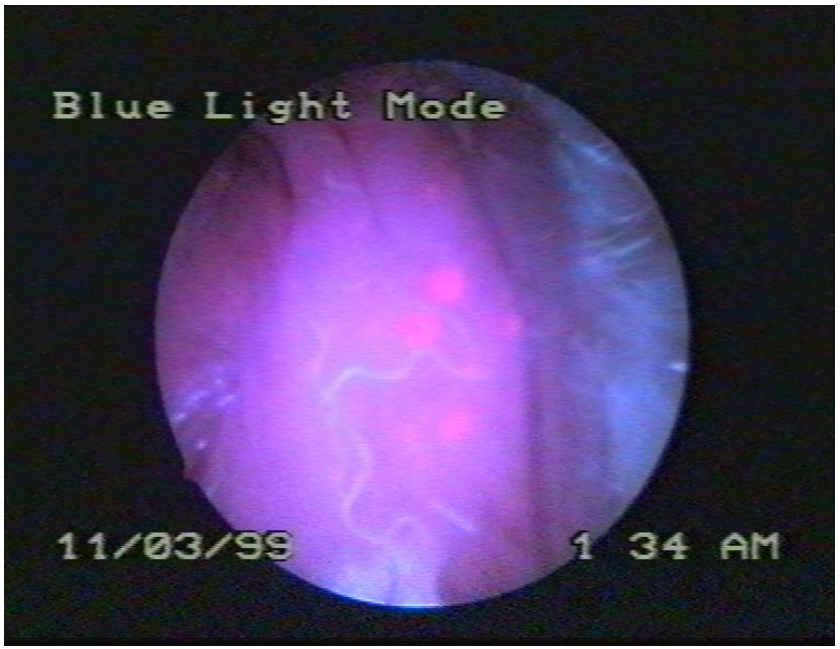


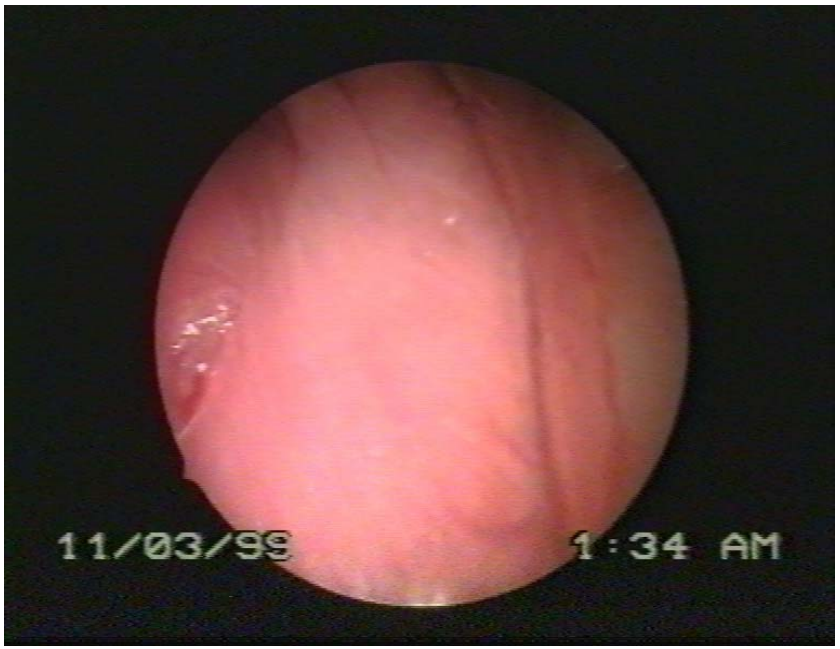

In vivo fluorescence and light images of peritoneal tumor nodules. Fluorescence was excited using an endoscope (with D-light) after ip administration of ALA in an ovarian cancer rat (Fischer 344) model.

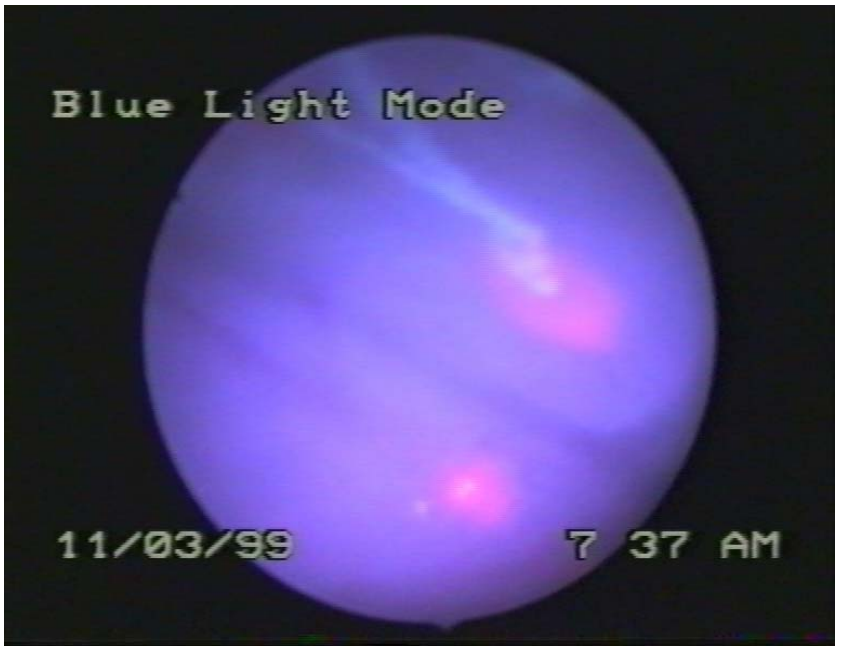


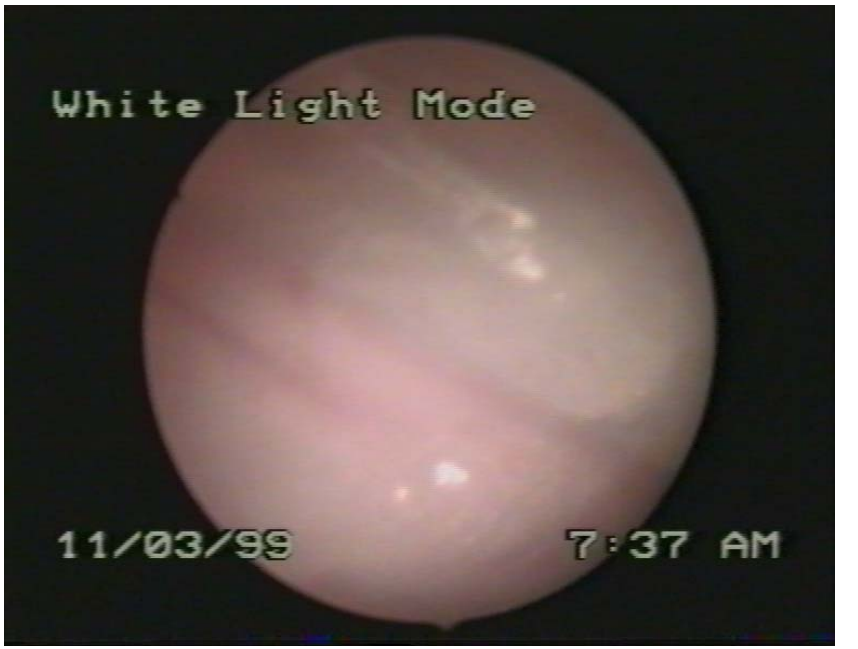

In vivo fluorescence and light images of peritoneal tumor nodules. Fluorescence was excited using an endoscope (with D-light) after ip administration of ALA in an ovarian cancer rat (Fischer 344) model.

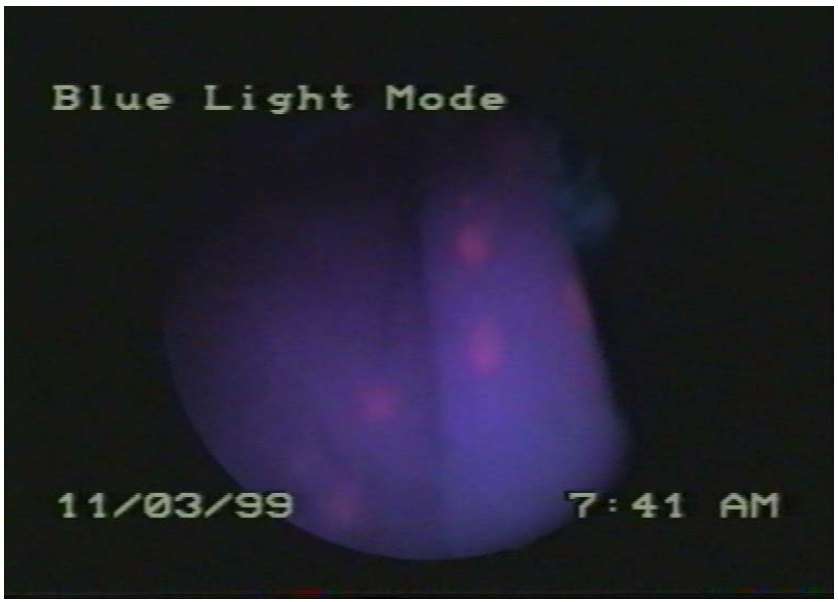


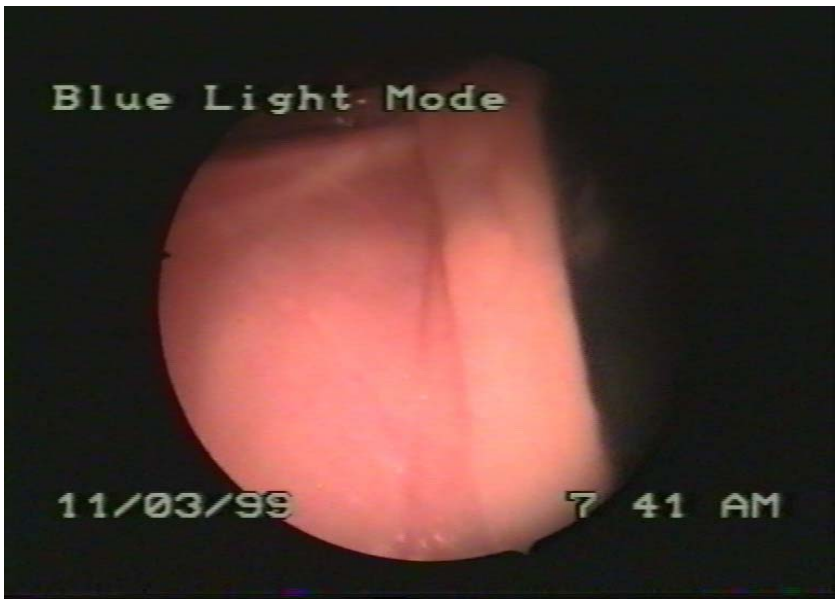

In vivo fluorescence and light images of peritoneal tumor nodules. Fluorescence was excited using an endoscope (with D-light) after ip administration of ALA in an ovarian cancer rat (Fischer 344) model.

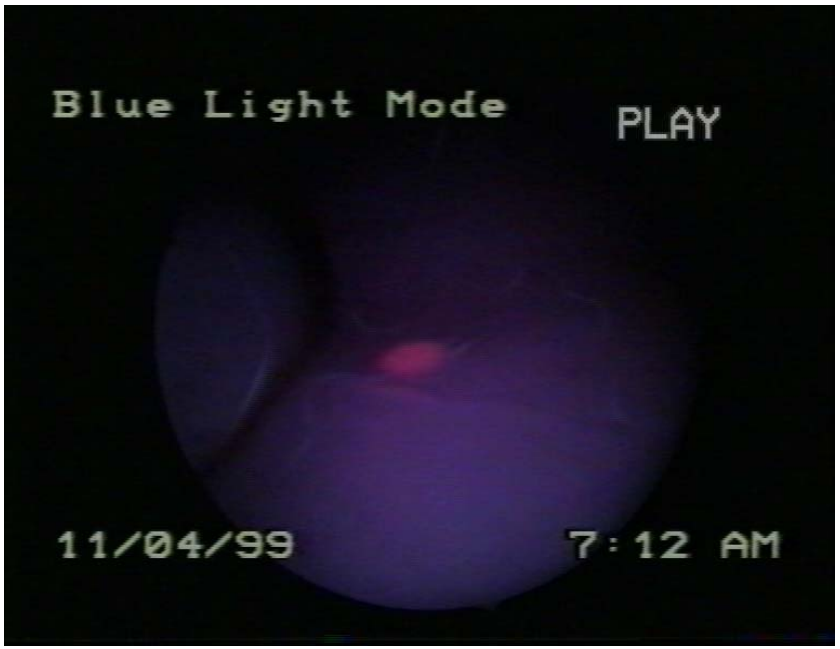


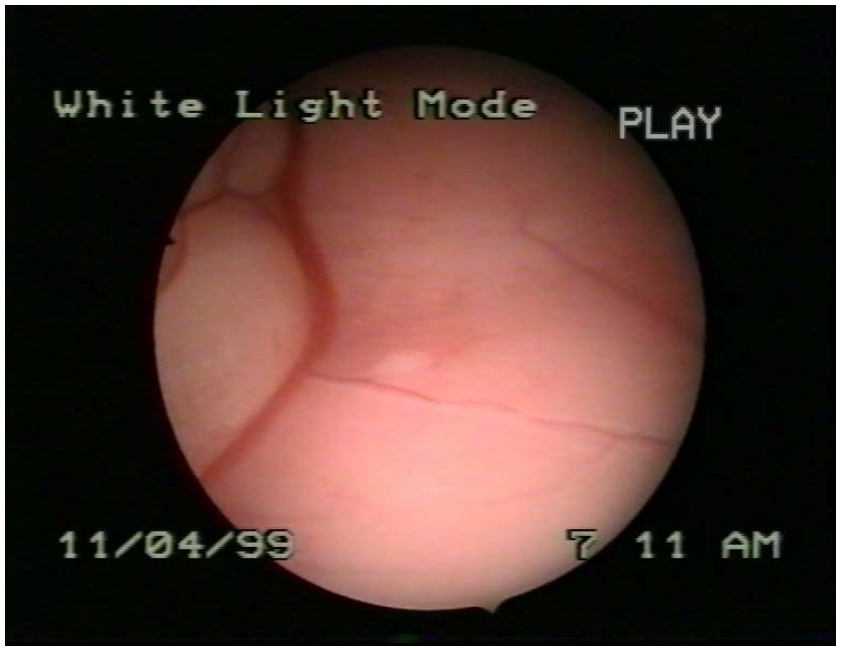

In vivo fluorescence and light images of peritoneal tumor nodules. Fluorescence was excited using an endoscope (with D-light) after ip administration of ALA in an ovarian cancer rat (Fischer 344) model.

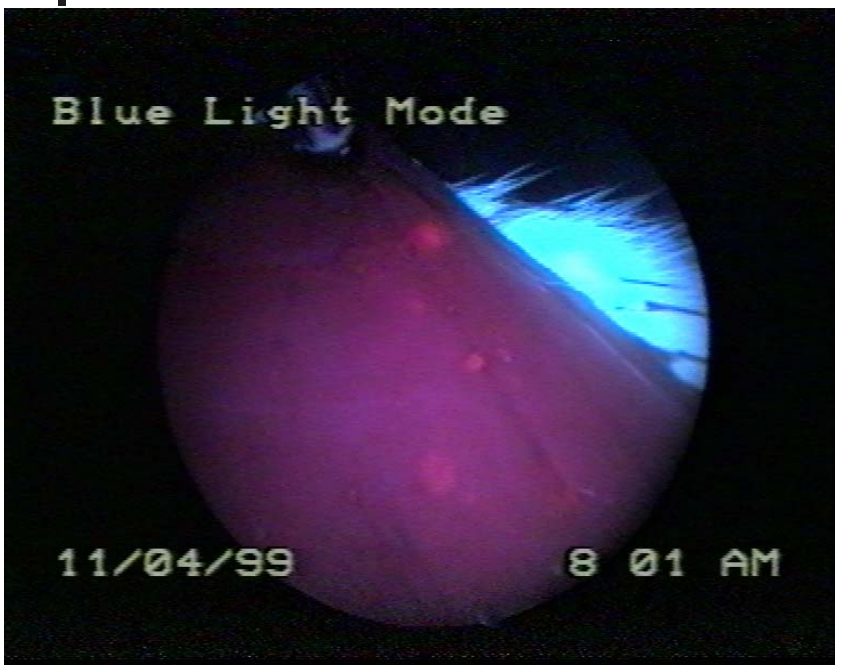


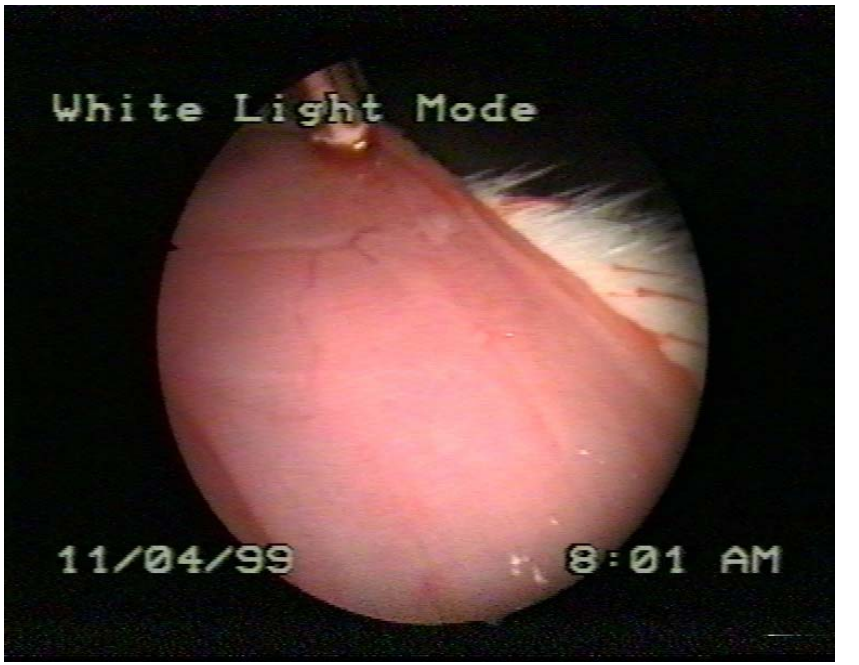

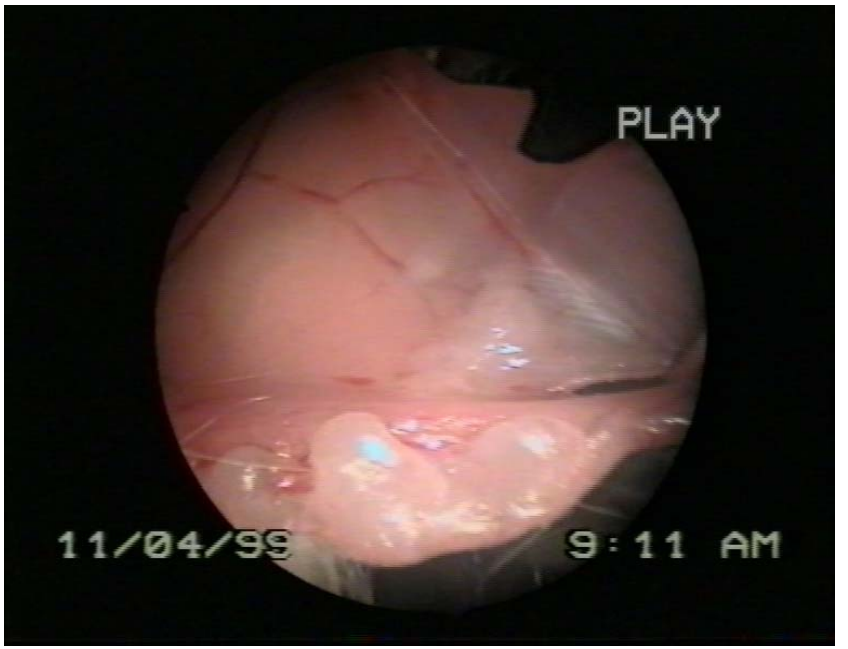
PLAY
11/04/99
9:11 AM

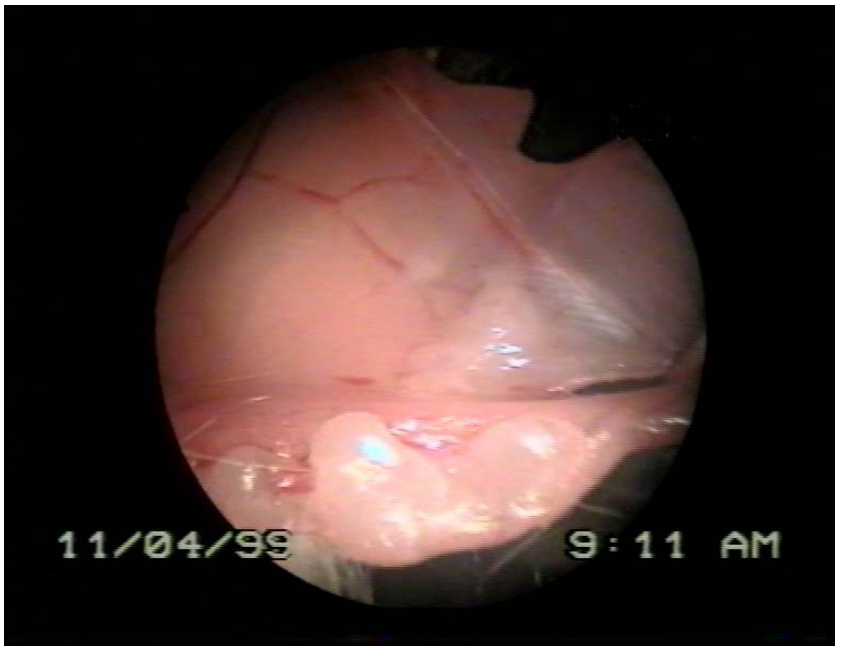
11/04/99
9:11 AM

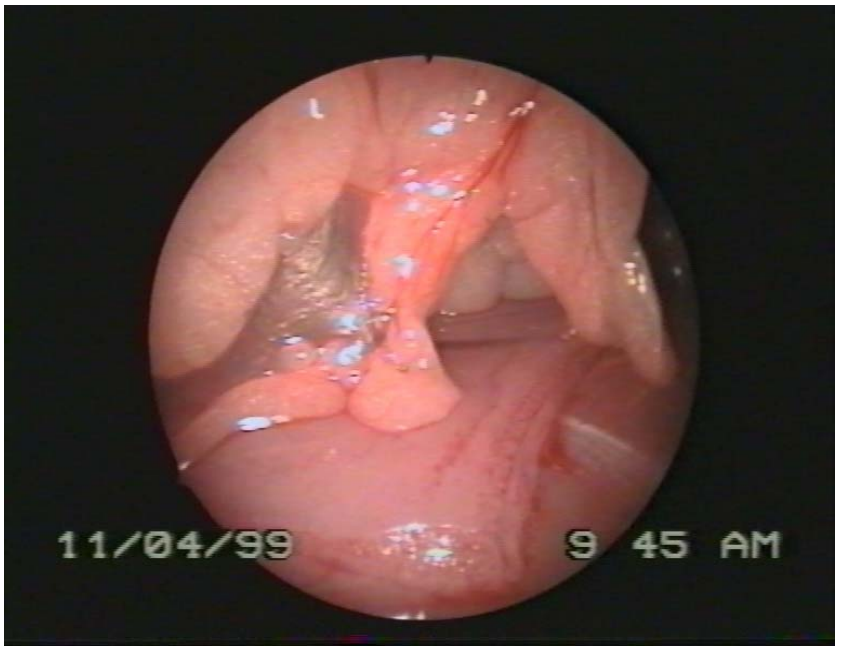
11/04/99
9 45 AM

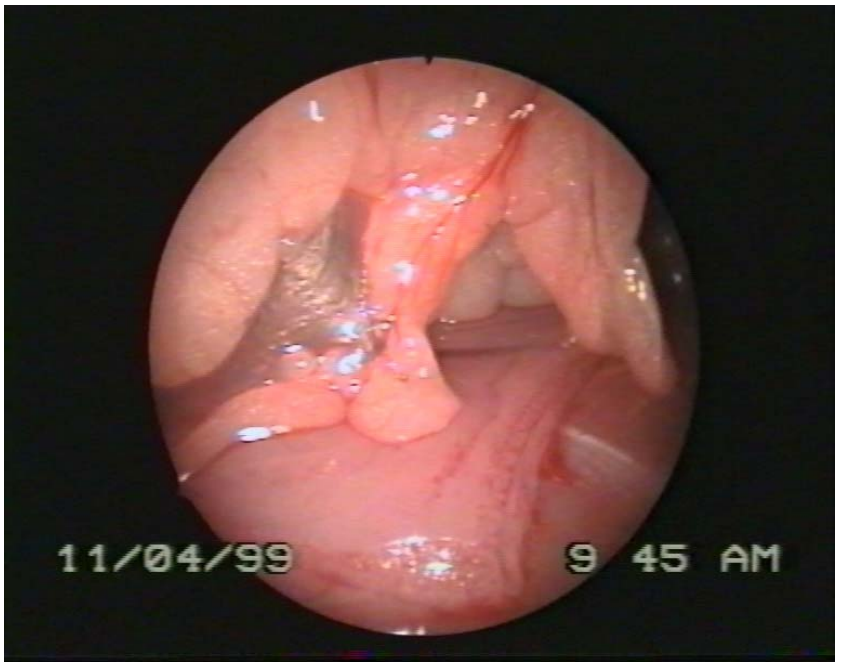
11/04/99
9 45 AM

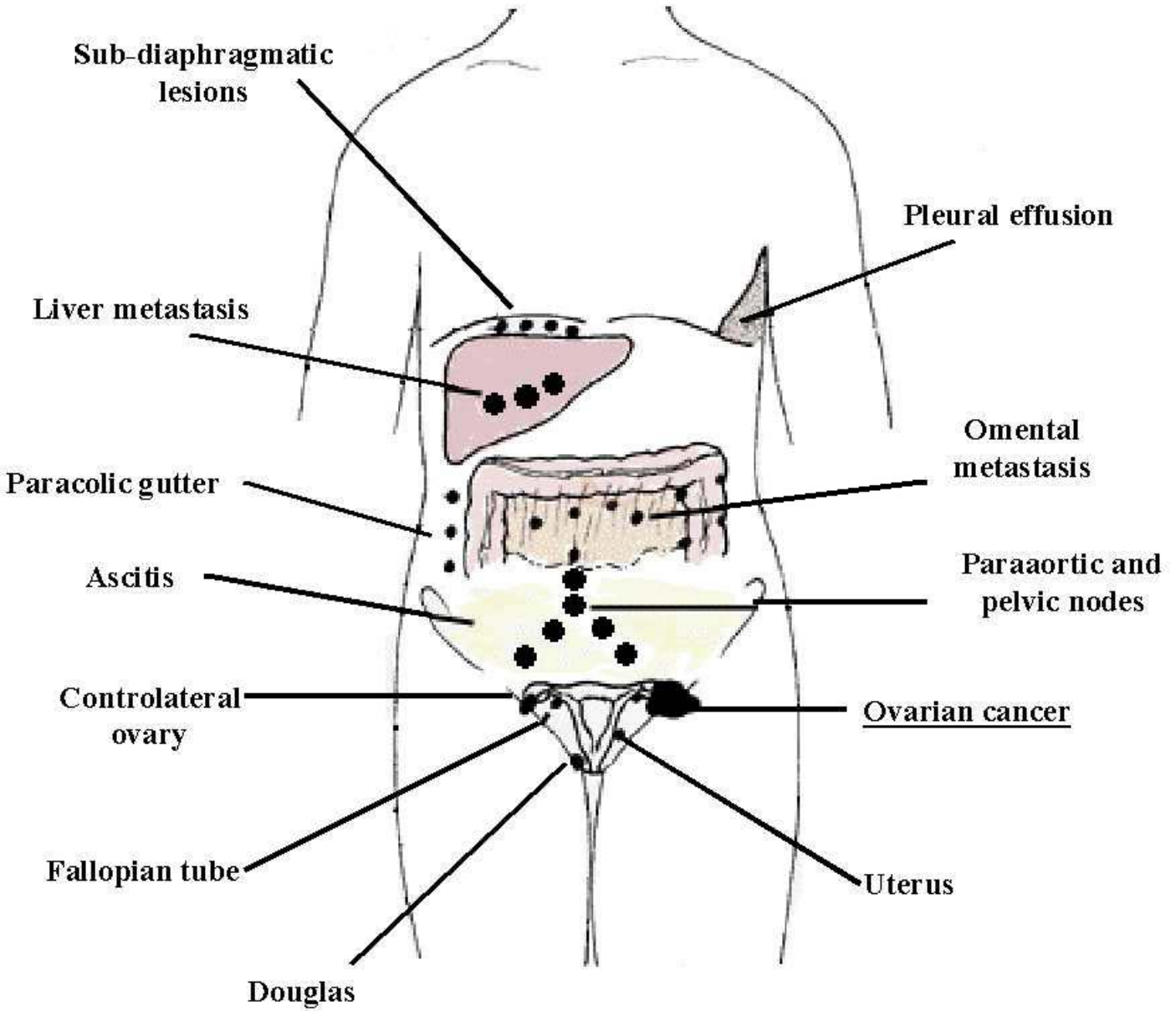
Sub-diaphragmatic lesions
Pleural effusion
Liver metastasis
Omental metastasis
Paracolic gutter
Paraaortic and pelvic nodes
Ascitis
Controlateral ovary
Ovarian cancer
Fallopian tube
Uterus
Douglas

# Fluorescence of Peritoneal Nodules 2.0 hours after i.p. injection

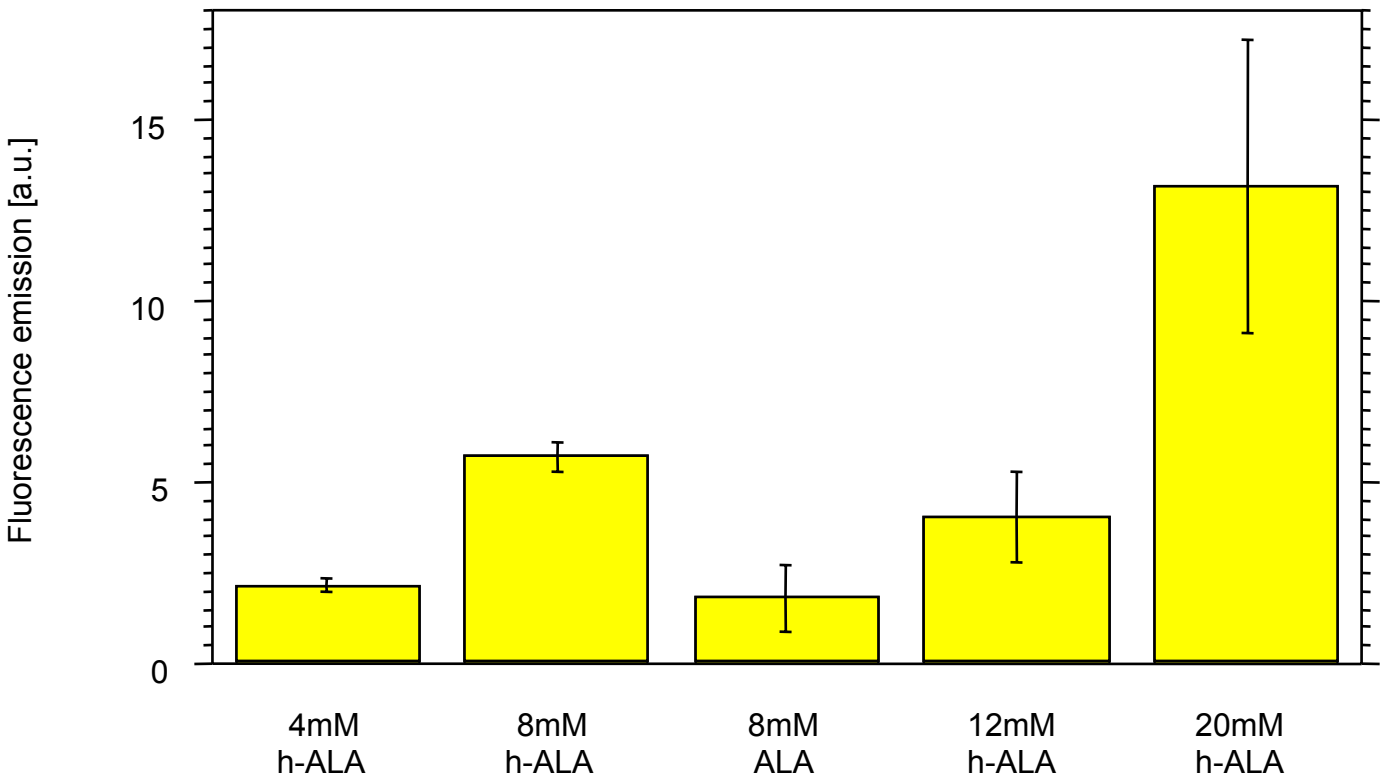

| Stage | | Description | 5-year survival Rate (%) |
|---|---|---|---|
| **1. I** | | **Growth limited to the ovaries** | **61** |
| | Ia | One ovary involved } no ascitis capsule intact | 65 |
| | Ib | Both ovaries involved } no ascitis capsule intact | 52 |
| | Ic | Ascites present, or positive peritoneal washing, tumor on the surface of the ovary | |
| **2. II** | | **Growth limited to pelvis** | **40** |
| | IIa | Extension to the uterus and the tubes | 60 |
| | IIb | Extension to other pelvic tissues | 38 |
| | IIc | Like Ic | |
| **3. III** | | **Growth extending to abdominal cavity, including peritoneal surface and omentum** | **5** |
| | IIIa | Microscopic abdominal implants, negative nodes | |
| | IIIb | Macroscopic abdominal implants, < 2 cm, negative nodes | |
| | IIIc | Abdominal implants > 2 cm and/or positive nodes | |
| **4. IV** | | **Metastases to distant sites (positive pleural cytology, parenchymal liver metastasis)** | **3** |

*The 5-year survival rate of ovarian Cancer in Geneva*

## *5-year cumulative lethality rate of gynecologic malignancies in Geneva*

| Interval | Cervix uteri | Corpus Uteri | Ovary | Other genital organs | Breast |
|---|---|---|---|---|---|
| 0-1st | 15.3% | 16.3% | 43.7% | 28.0% | 9.1% |
| 0-2nd | 27.3% | 25.2% | 59.9% | 38.7% | 16.1% |
| 0-3th | 33.3% | 30.6% | 67.8% | 40.9% | 23.7% |
| 0-4th | 38.2% | 34.5% | 71.1% | 47.3% | 30.2% |
| 0-5th | 42.3% | 37.6% | 72.2% | 52.7% | 35.1% |

*data from Geneva 1970-1994*

# Comparative rate (Europe) per 100'000 population per year

*Year specific mortality curve of genital malignancies, Geneva 1970-1994*

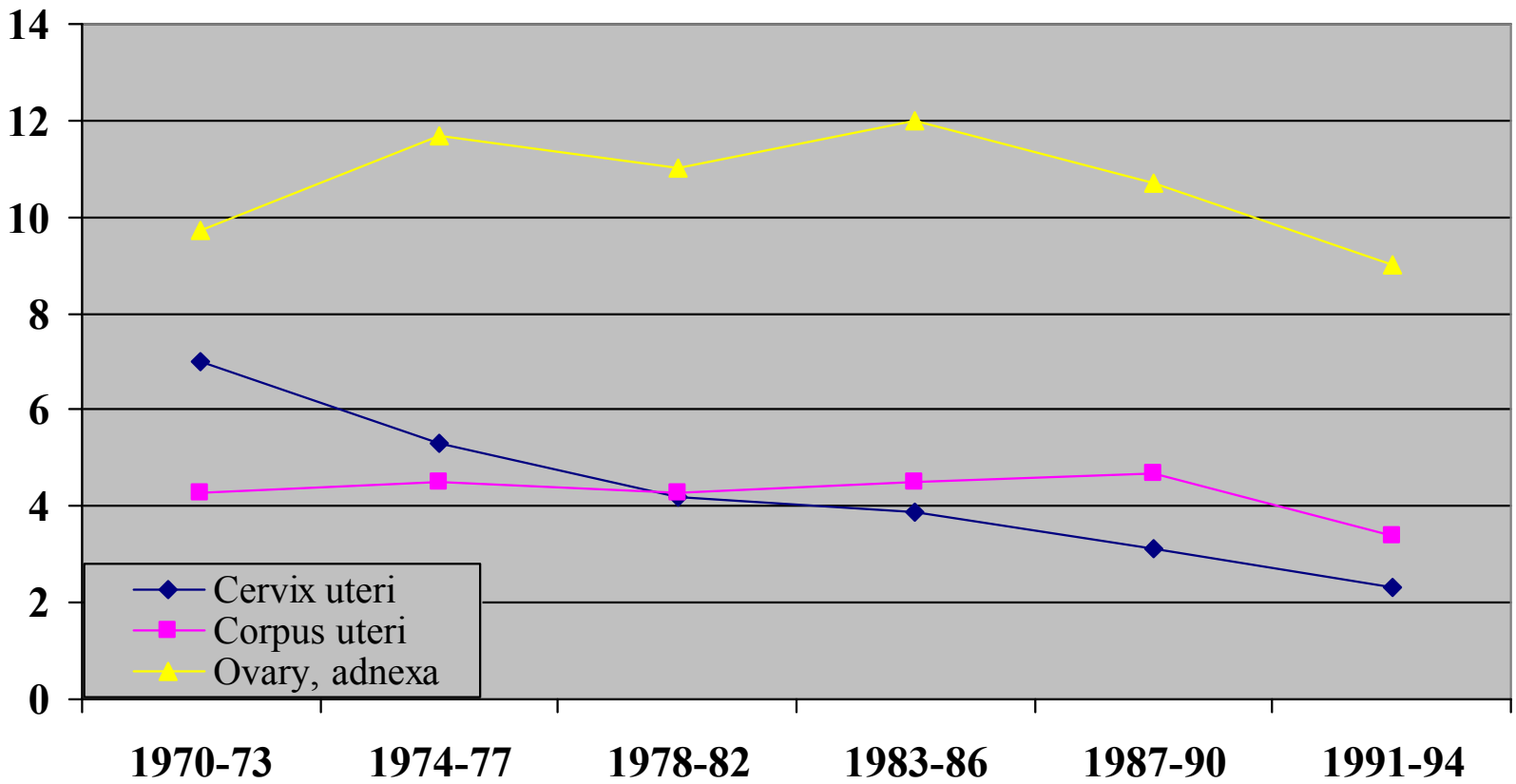

# Pp IX Spectrum measured on Peritoneal Nodule

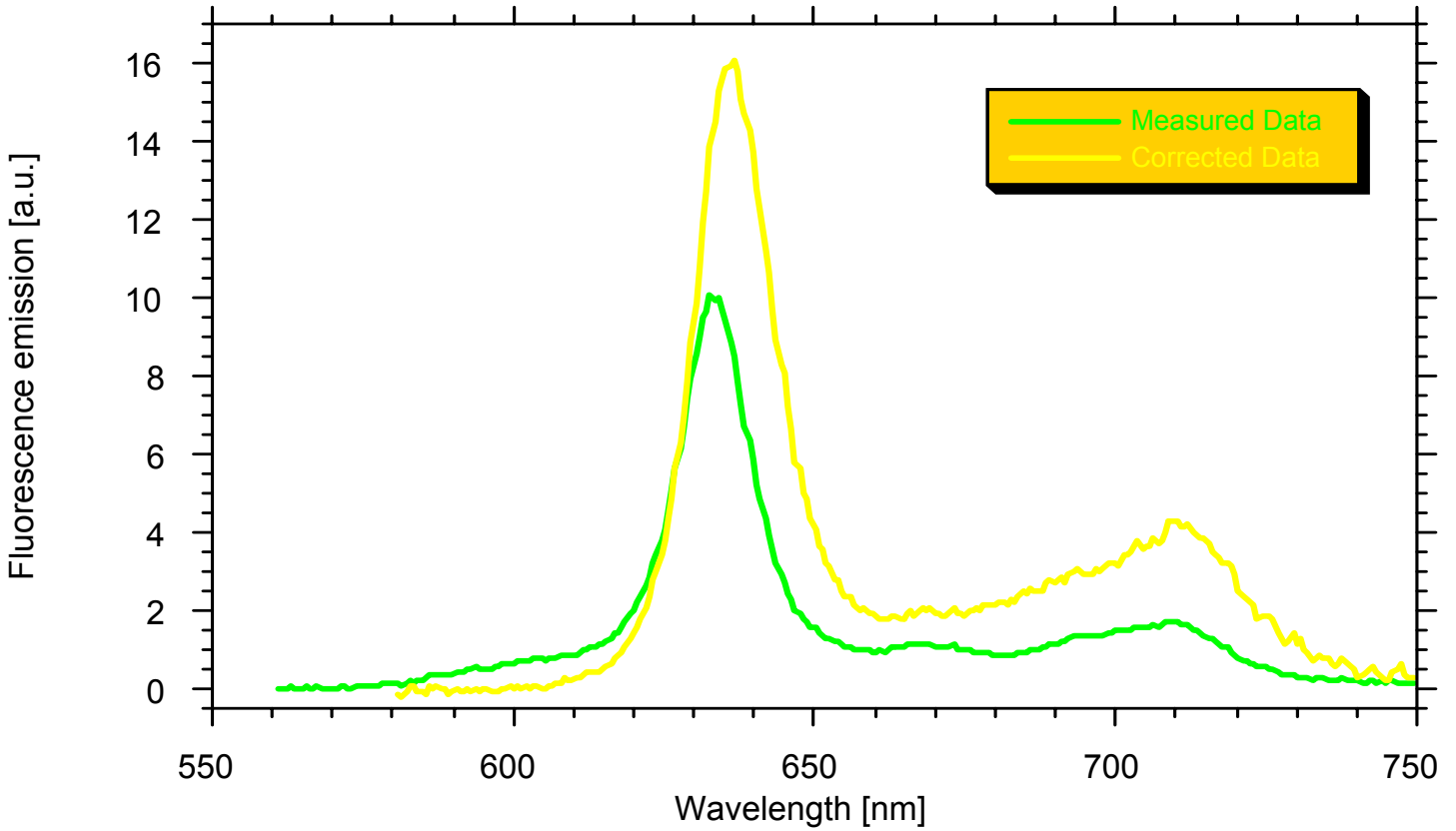

# *Scattering and refraction of light*

Rayleigh scattering

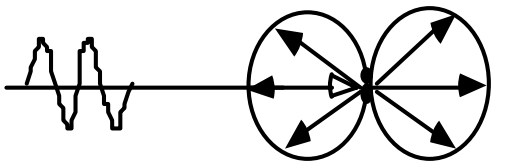

Mie scattering

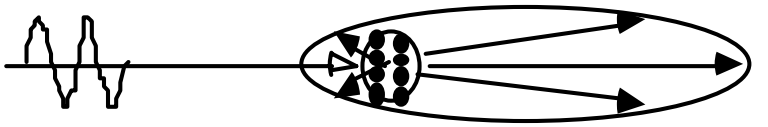

Refraction

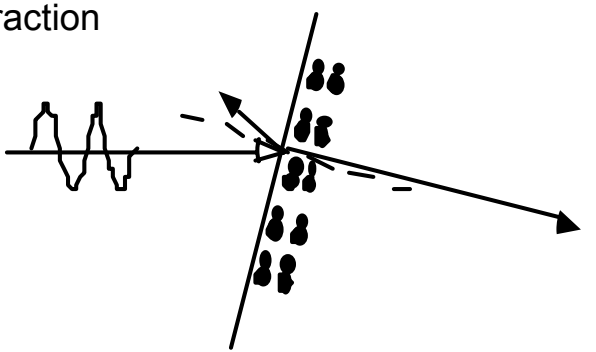

# Light propagation

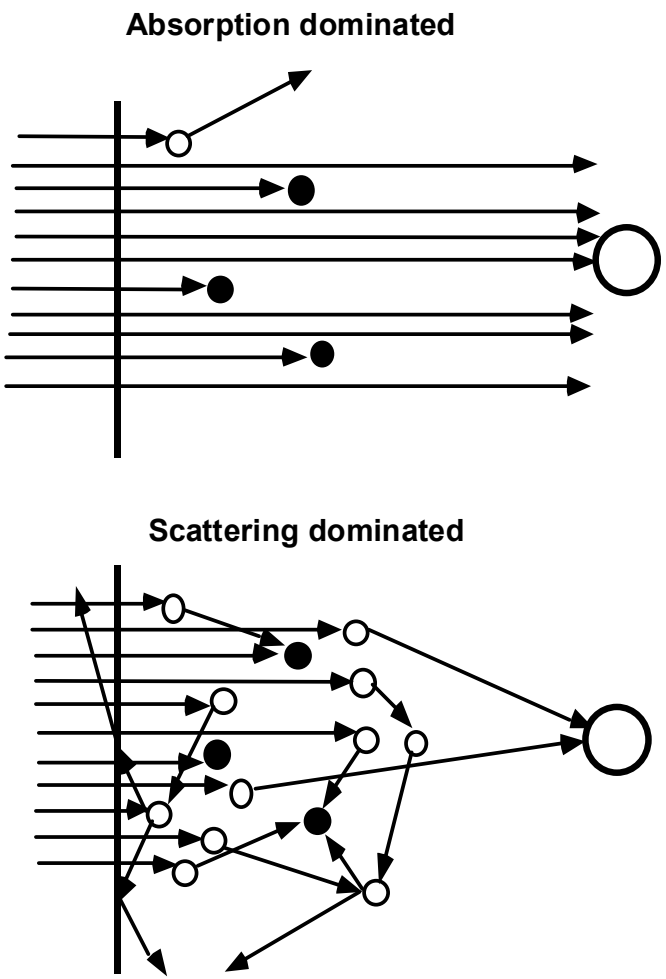


*Light propagation in absorption dominated and in scattering dominated tissues. Small solid and open circles represent absorbers and scatterers, respectively. Larger open circles represent target molecules.*

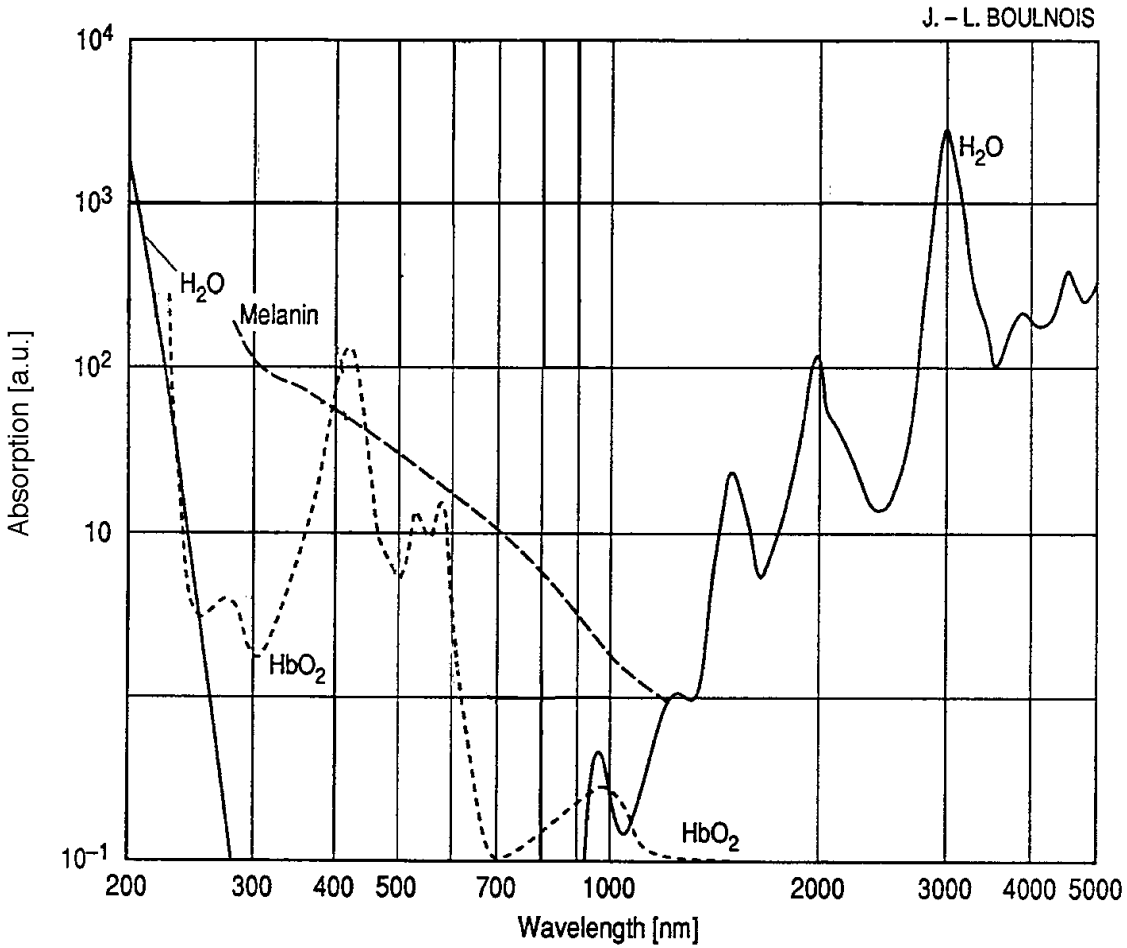


Absorption of water, melanin (broken line) and oxyhemoglobin ($HbO_2$) (dotted line)

# Penetration depth of light in tissue in relation to the wavelength

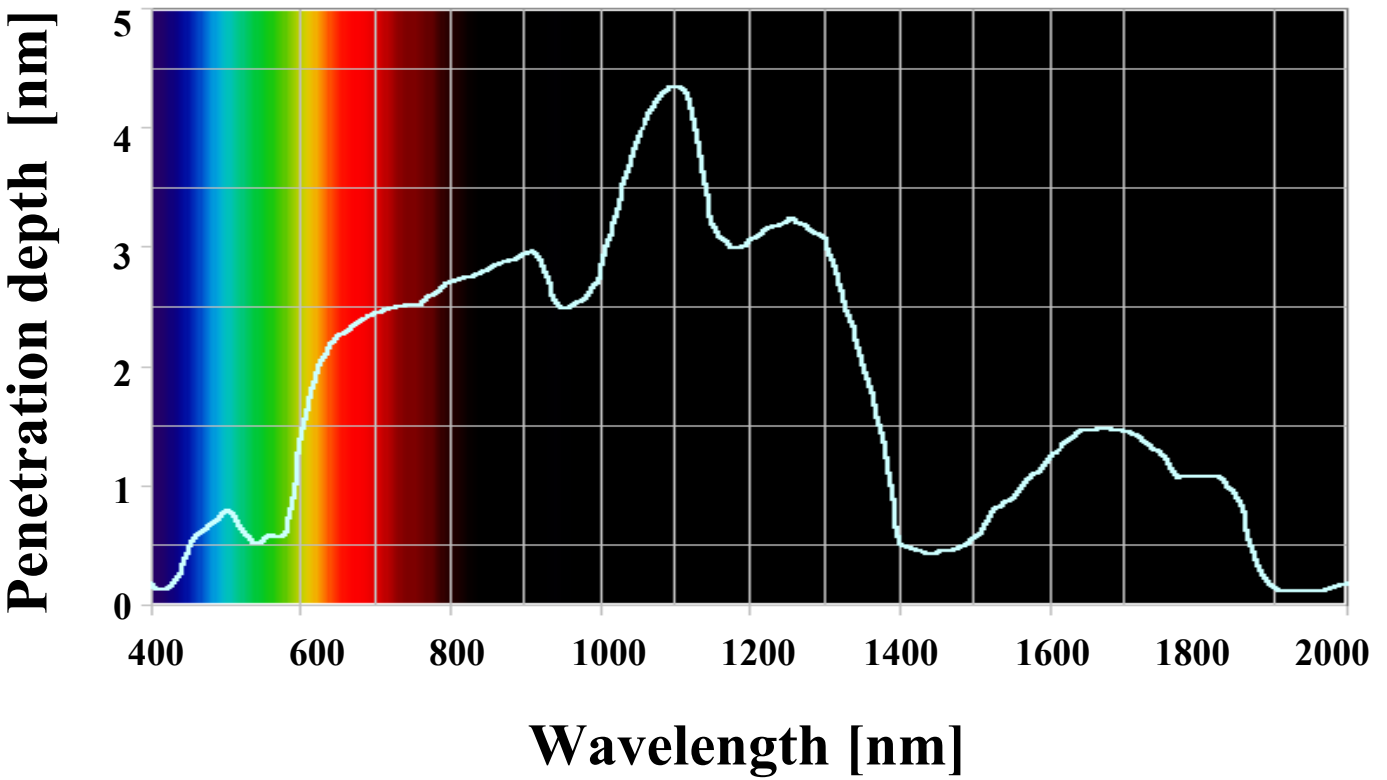

# Excitation of photosensitizer and singlet oxygen generation

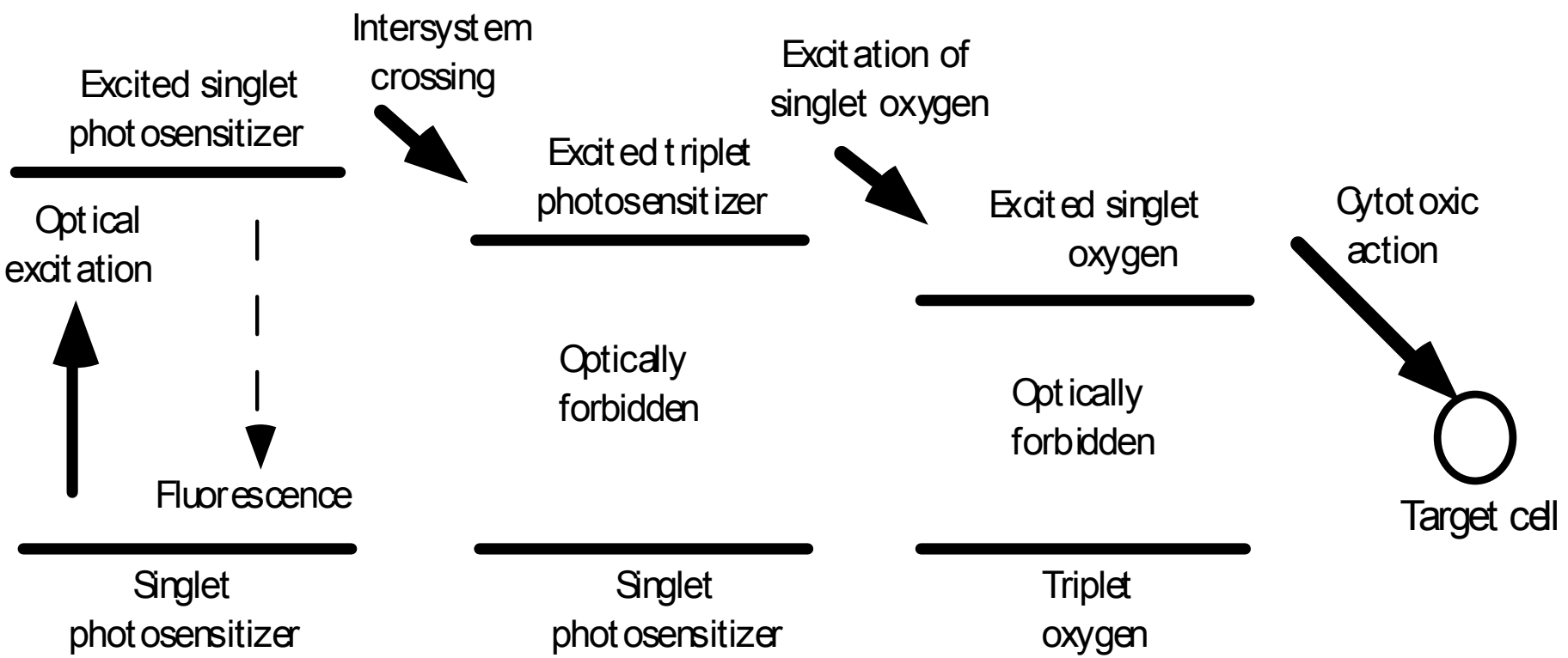

# Chemical structure of 5-ALA and PpIX. Me represents methyl group

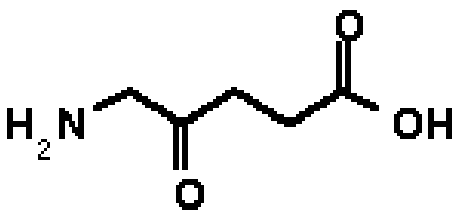


5-ALA

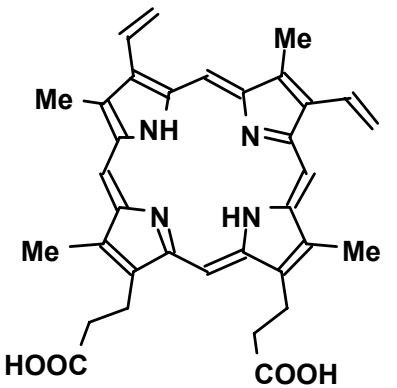

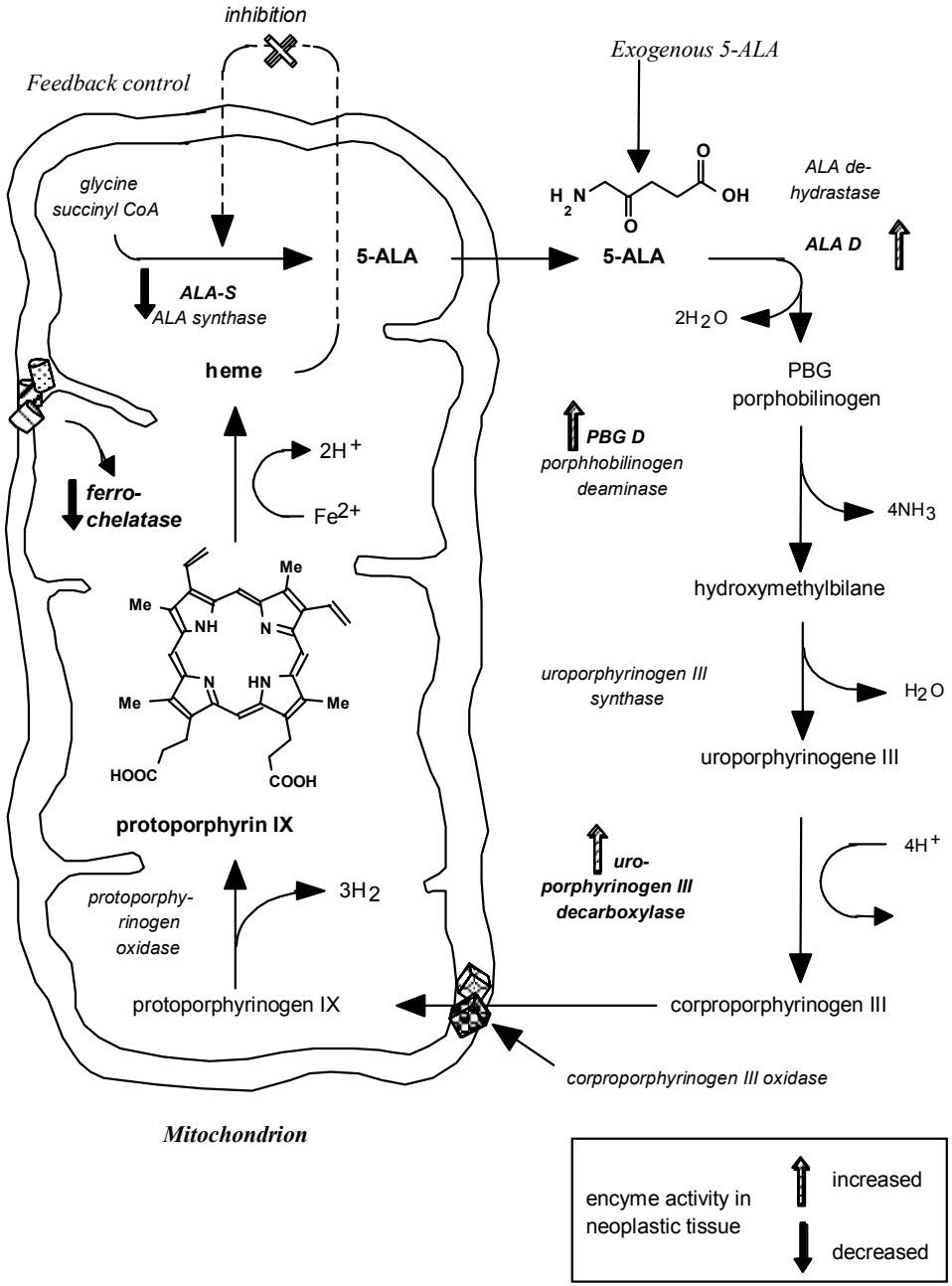
inhibition
Feedback control
Exogenous 5-ALA
glycine
succinyl CoA
5-ALA
5-ALA
ALA-S
ALA synthase
ALA de-
hydrastase
ALA D
2H2O
heme
PBG
porphobilinogen
PBG D
porphhobilinogen
deaminase
2H+
Fe2+
ferro-
chelatase
4NH3
hydroxymethylbilane
uroporphyrinogen III
synthase
H2O
uroporphyrinogene III
protoporphyrin IX
4H+
uro-
porphyrinogen III
decarboxylase
protoporphy-
rinogen
oxidase
3H2
protoporphyrinogen IX
corproporphyrinogen III
corproporphyrinogen III oxidase
Mitochondrion
encyme activity in
neoplastic tissue
increased
decreased

Absorption (blue line) and fluorescence (pink line) spectrum of PpIX solved in DMSO. Values of absorption and fluorescence do not correspond to each other

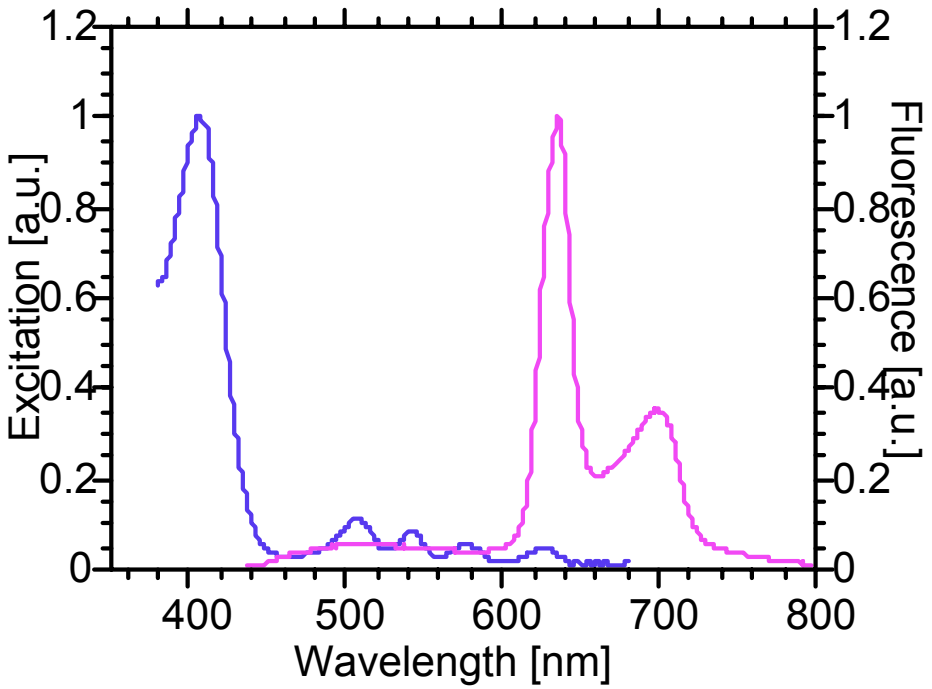

# *Set up of the optical fiber based spectrofluorometer*

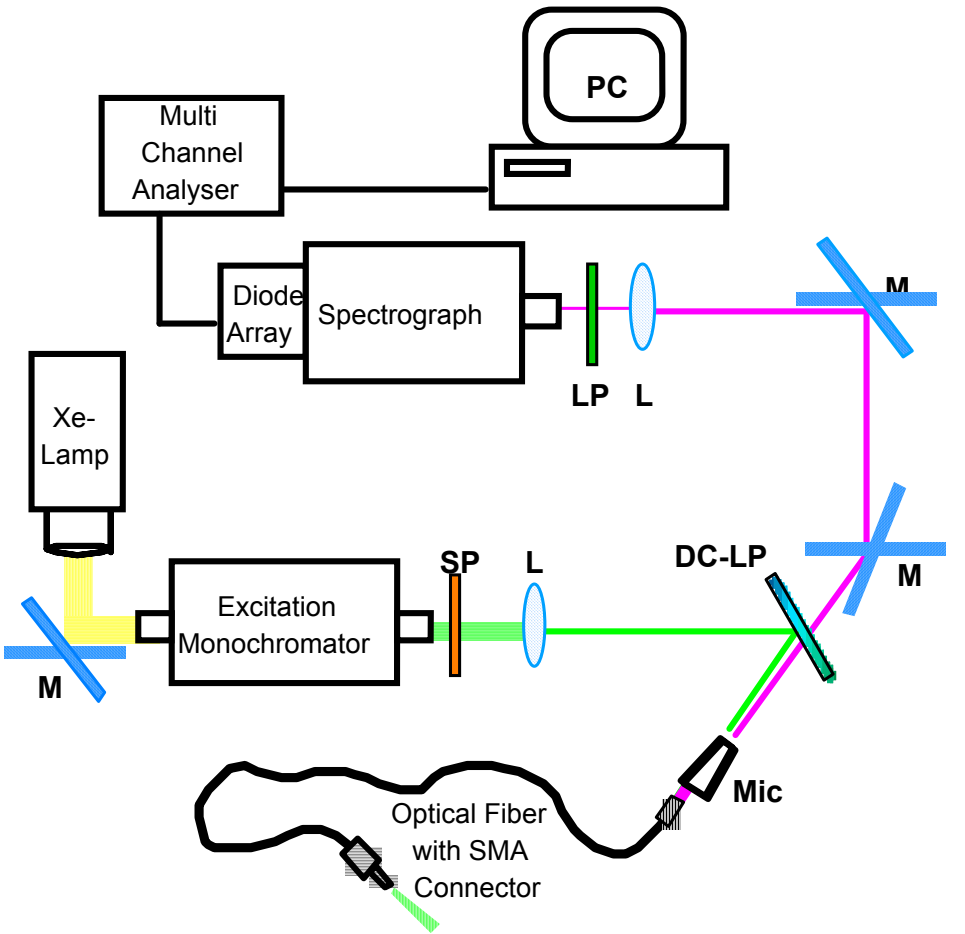

## Drug Injection Data: the table shows the total number of rats, the injected drug, the drug dose and the time delay between injection and measurement

| Number of Rats | Drug | Concentration | Time |
|---|---|---|---|
| 1 | h-ALA | 4mM | 2.0 h |
| 2 | h-ALA | 4mM | 2.5 h |
| 1 | h-ALA | 8mM | 0.5 h |
| 1 | h-ALA | 8mM | 1.0 h |
| 1* | h-ALA | 8mM | 1.5 h |
| 4 | h-ALA | 8mM | 2.0 h |
| 2 | h-ALA | 12mM | 2.0 h |
| 2* | h-ALA | 12mM | 2.5 h |
| 2* | h-ALA | 20mM | 2.0 h |
| 2 | ALA | 8mM | 2.0 h |

# Reference signal

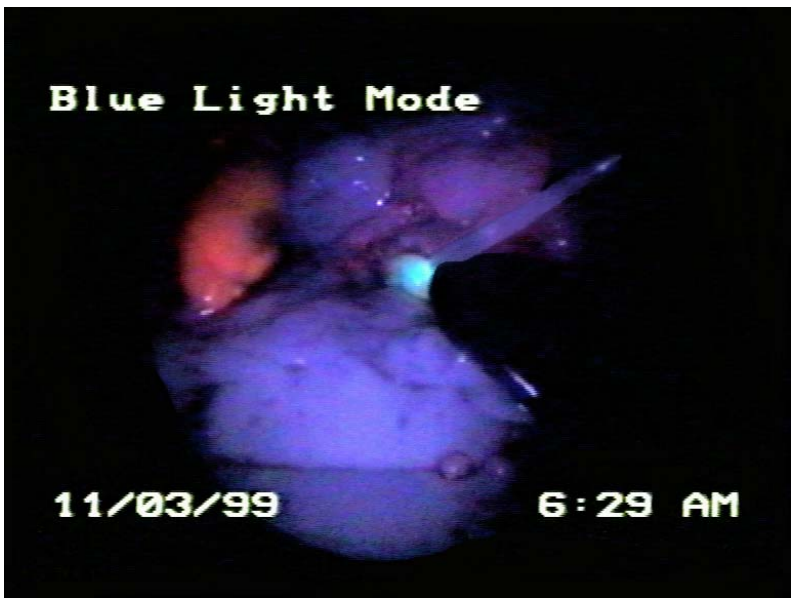


Optical fiber in measuring position on the omentum; the red fluorescing tissue at the “10-o’clock” position shows a part of the fluorescing intestine

## D-Light Inspection

- After spectrometric measurements the abdomen was inspected with the Storz D-Light system. The quantities and settlings of the metastases that could be observed in the white and blue light mode, respectively, were noted. Moreover pictures of the metastases in white light and blue light were recorded by the video system.

# Fluorescence metastases in dependence on drug concentration

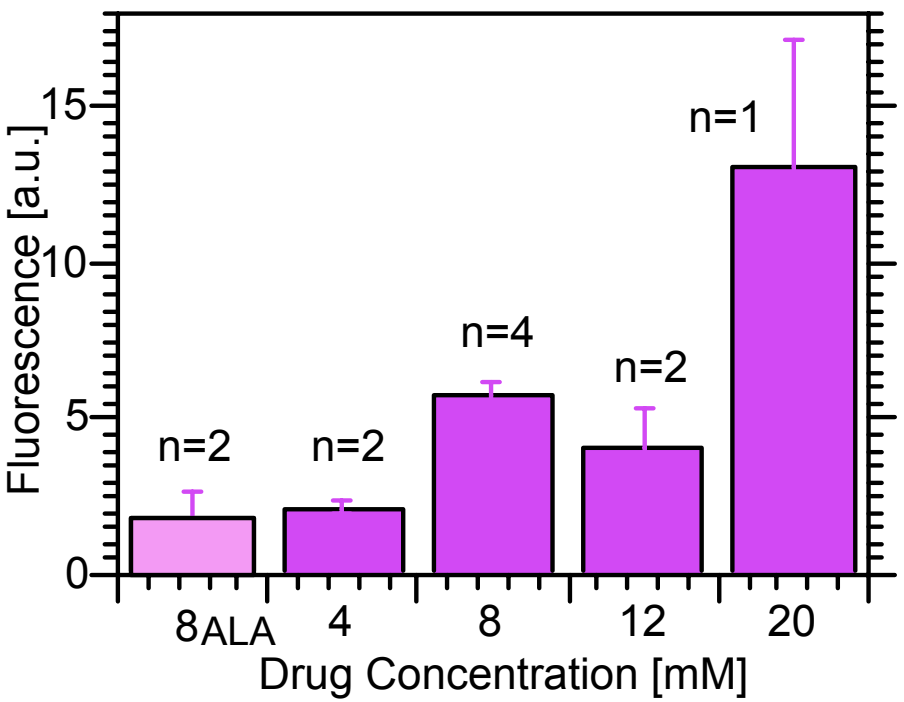


Fluorescence of peritoneal nodules in dependence on drug concentration 2 to 2.5 h after drug injection; if not noted otherwise values give concentration of h-ALA, n depicts the number of rats

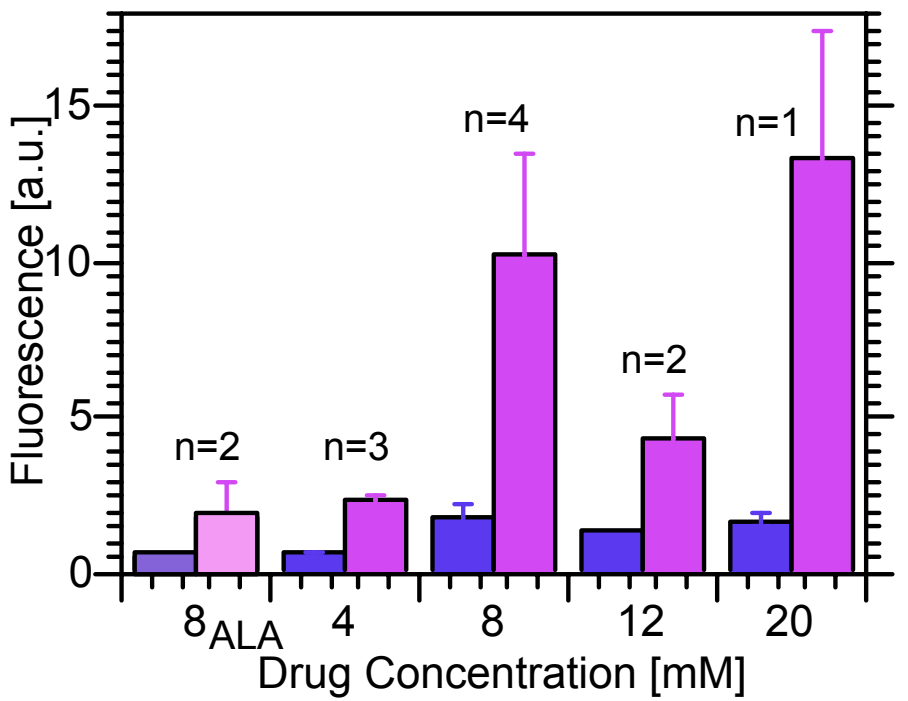


*Fluorescence emission of healthy (blue) and nodular tissue (violet)*

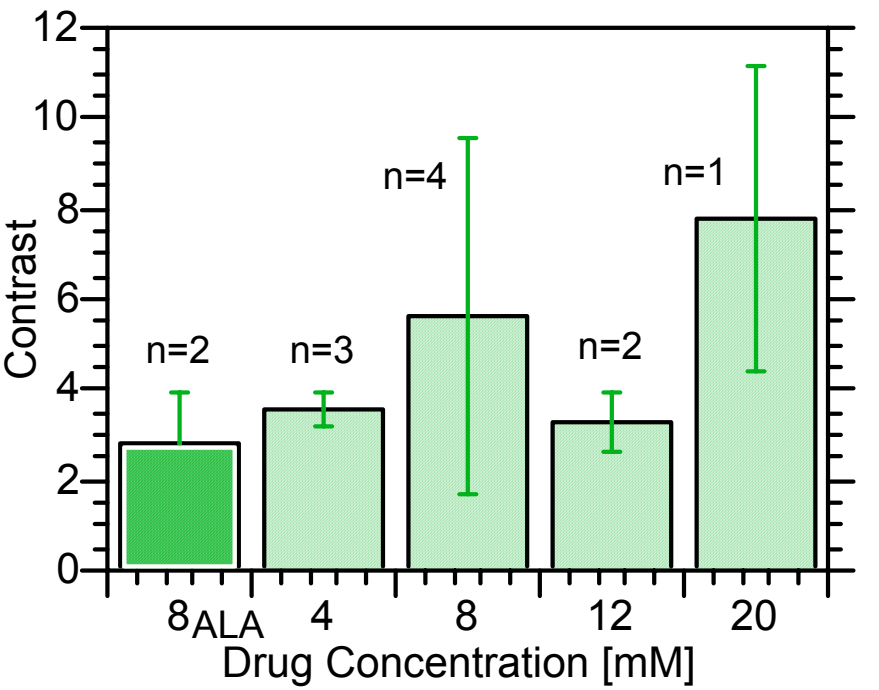


*Physical contrast C of nodular to healthy tissue for different concentrations of ALA and h-ALA*

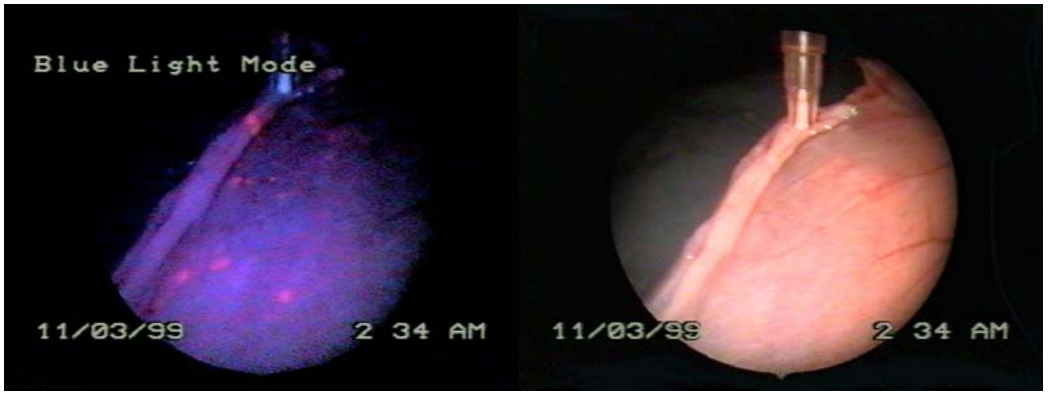


***A***

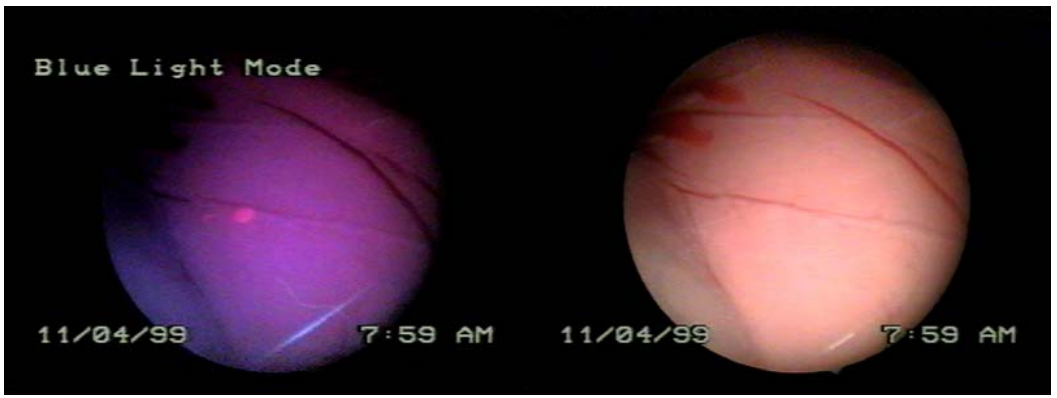


***B***

Blue and white light mode images of peritoneal nodules taken 2.0 hours after i.p.injection of 8mM (A) and 20mM (B) h-ALA, respectively. The blue light image B shows clearly the high red fluorescence of the healthy tissue that turned out to be difficult for detection of very small nodules. On the other hand, fluorescence of the big nodule in picture B is higher than in the nodules shown in picture A.

# Time-dependence of nodule -fluorescence and fluorescence of healthy peritoneal tissue (dotted line) emission in rats injected with 8 mM h-ALA

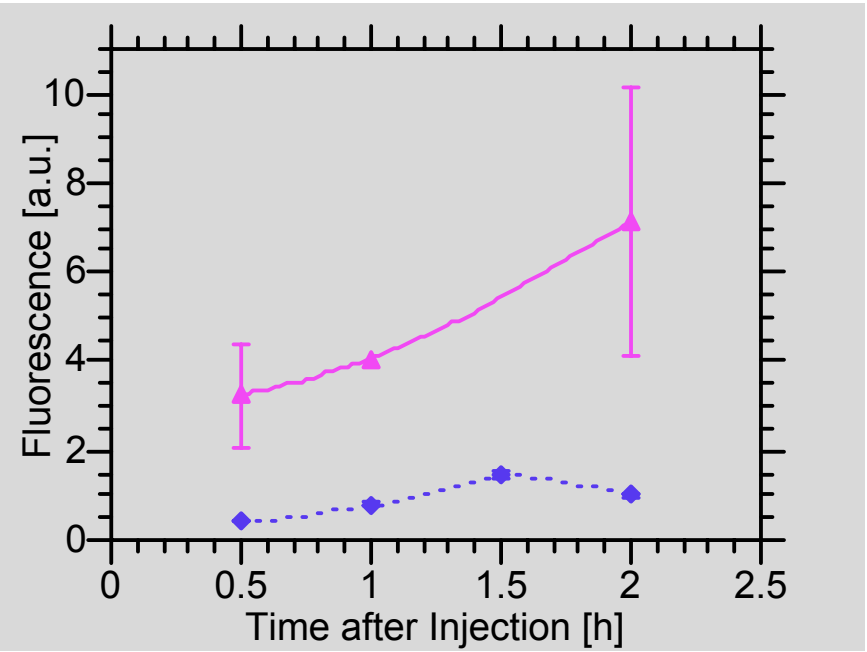


Information on time-dependence of the generation of PpIX was obtained from 7 rats injected with 8mM h-ALA. Fluorescence emission from the nodules and healthy tissue was acquired by spectrometer and the peritoneal sites were inspected with the D-Light system.

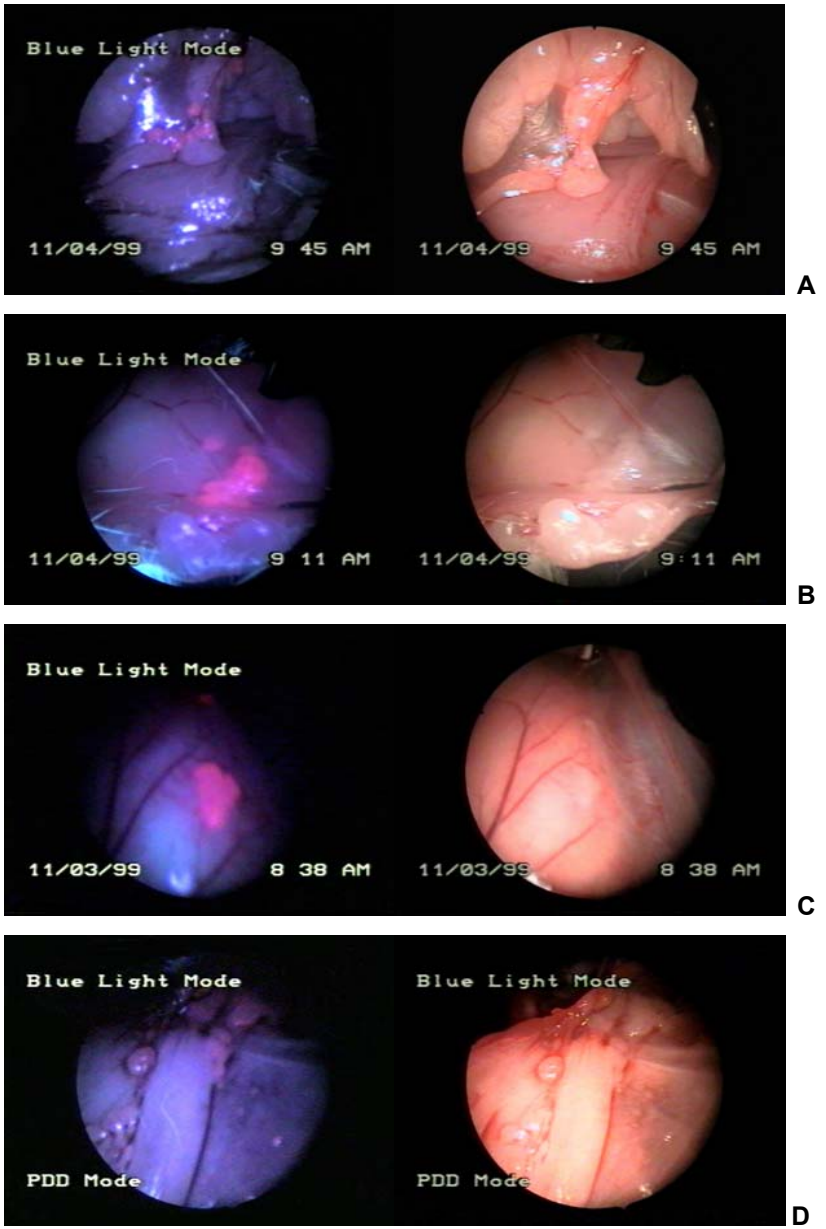


Blue and white light mode images of peritoneal nodules in rats sensitized with 8mM h-ALA taken at 0.5 (A), 1.0 (B) and 2.0 (C) hours after i.p. injection respectively. The increase of nodule fluorescence with time is apparent. Fluorescence achieved with ALA with a time delay of 2 h is comparable with that achieved with the same dose h-ALA after 0.5 h (D).

| Concentration [mM] | Time after inst. | White light | Bluelight | Ratio |
|---|---|---|---|---|
| 4 | 2.5 | 9 | 19 | 2.1 |
| 4 | 2.5 | 0 | 4 | 8 |
| 8 | 2.0 | 21 | 37 | 1.8 |
| 8 | 2.0 | 36 | 57 | 1.6 |
| 8 | 2.0 | 13 | 29 | 2.2 |
| 8 | 2.0 | 4 | 24 | 6 |
| 12 | 2.0 | 3 | 8 | 2.7 |
| 20 | 2.0 | 9 | 25 | 2.8 |
| 8 ALA | 2.0 | 10 | 16 | 1.6 |

Numbers of metastases detected with white and blue light detection for different concentrations of h-ALA and ALA. The ratio of nodules detected in blue light to those detected with white light exceeds 1.6 for all drugs and all concentrations

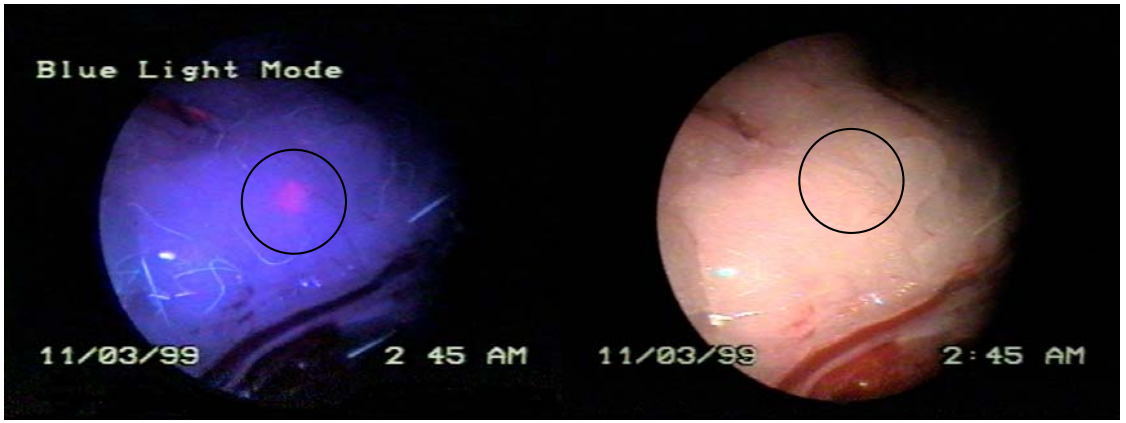


A

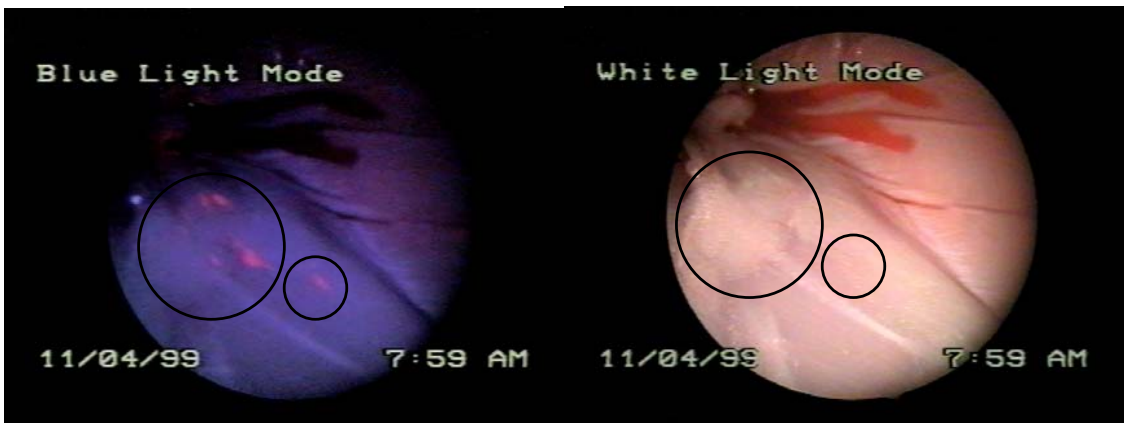


B

Images of peritoneal metastases in blue and white light mode: image A shows a lesion that is only visible in the blue light mode, but not with white light (position marked by a circle), (8mM h-ALA after 2.0h). Image B shows three lesions visible in blue and white light (big circle) and one only detectable by fluorescence (small circle) (20mM, 2.0h)

# *Small intestine*

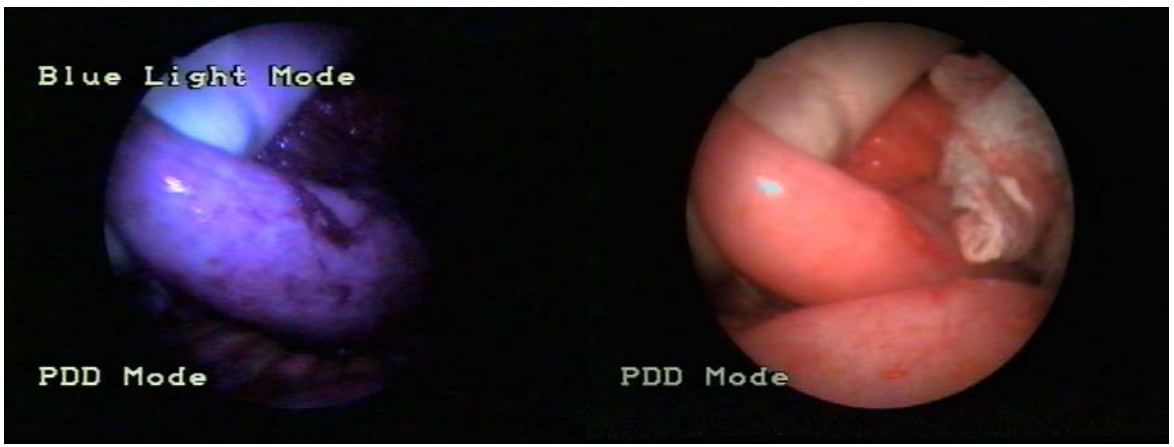


Blue and white light images of the small intestine. The human intestine shows no native PpIX fluorescence that was observed in the digestive organs of the rats.

## Conclusion

- The photosensitizer precursor Aminolaevulinic Acid hexylester (h-ALA) is suitable to detect micrometastases by means of photodiagnosis in the ovarian cancer animal model. Administered at the same dosage of 8 mmol and applied during the same time interval h-ALA results in higher PPIX fluorescence emission than its counterpart ALA. The clinical impact of these findings remain to be shown.

# Fluorescence of Pax, Theil and Mouth Mucosa 2 hours after i.p. injection

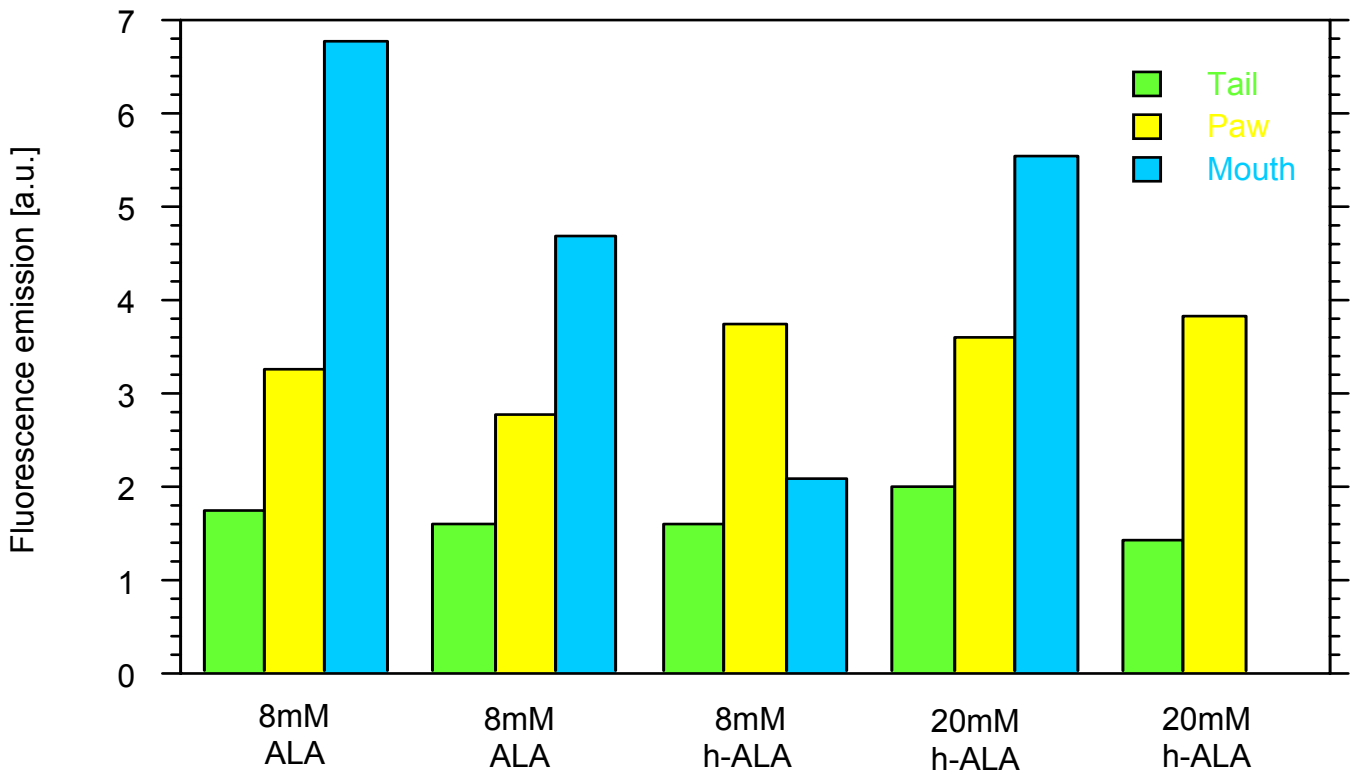

# Cervical cancer in situ tendancy in Geneva

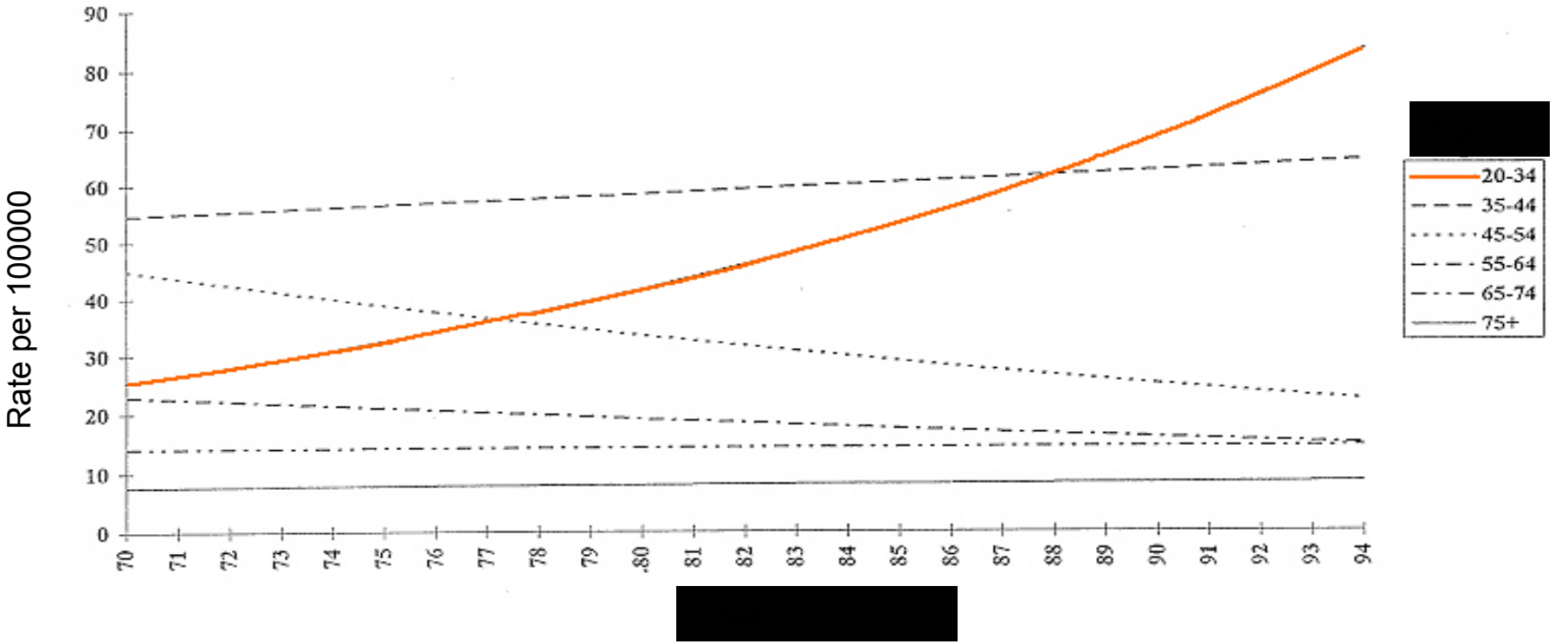


*Tumor Registry of Geneva, May 1996*

# Block diagram of the Cancer Photodetection apparatus

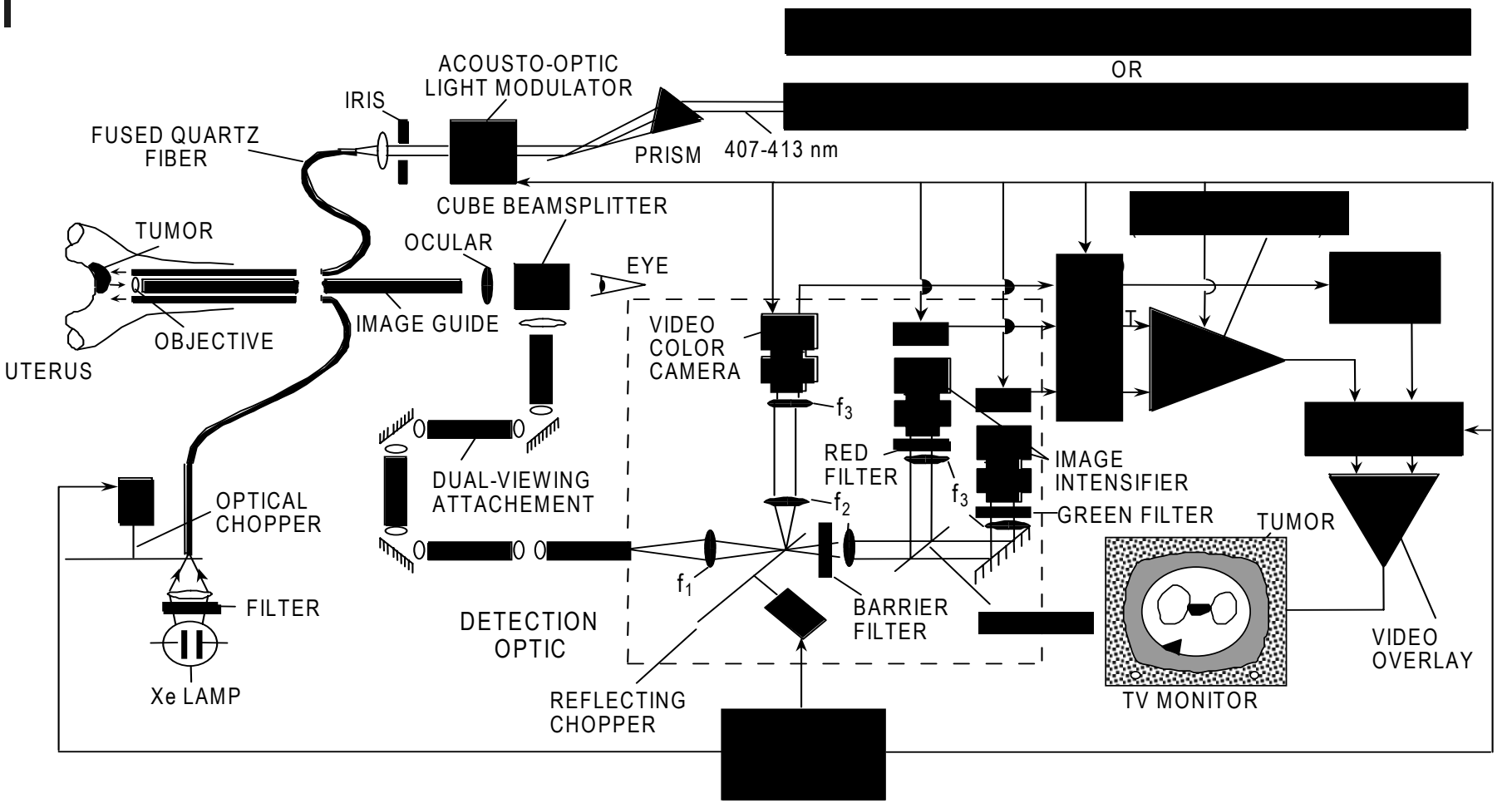

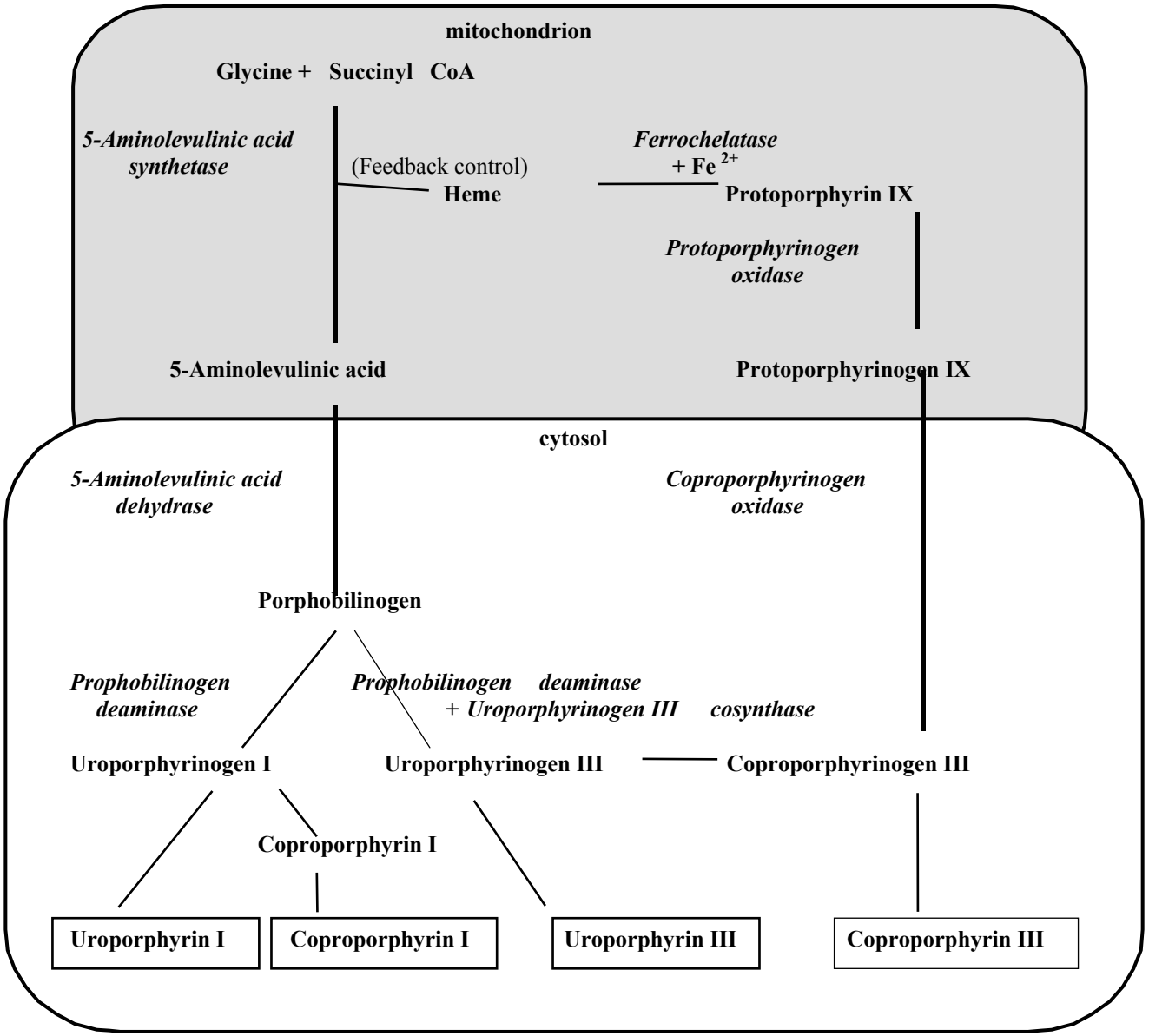
mitochondrion
Glycine + Succinyl CoA
5-Aminolevulinic acid synthetase
(Feedback control)
Heme
Ferrochelatase
+ Fe 2+
Protoporphyrin IX
Protoporphyrinogen oxidase
5-Aminolevulinic acid
Protoporphyrinogen IX
cytosol
5-Aminolevulinic acid dehydrase
Coproporphyrinogen oxidase
Porphobilinogen
Prophobilinogen deaminase
Prophobilinogen deaminase
+ Uroporphyrinogen III cosynthase
Uroporphyrinogen I
Uroporphyrinogen III
Coproporphyrinogen III
Coproporphyrin I
Uroporphyrin I
Coproporphyrin I
Uroporphyrin III
Coproporphyrin III

# Cervicoscopy after topical ALA application

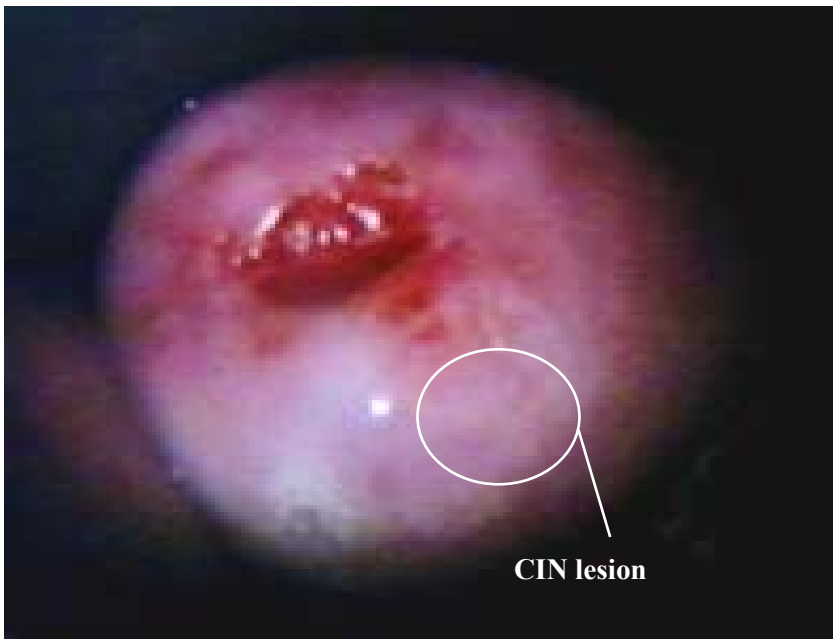


Cervix white light examination

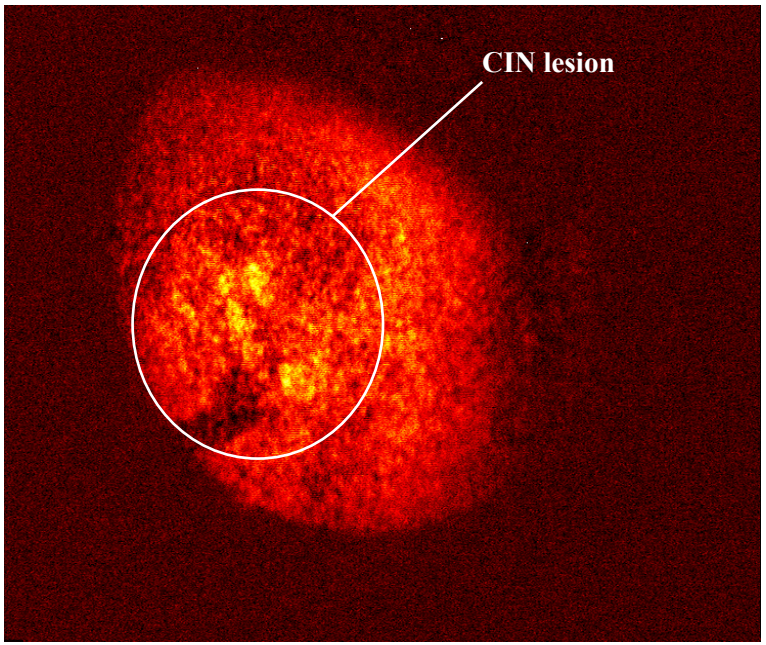


Cervix fluorescence under TDP (green-bleu)

# HE and Fluorescence microscopy

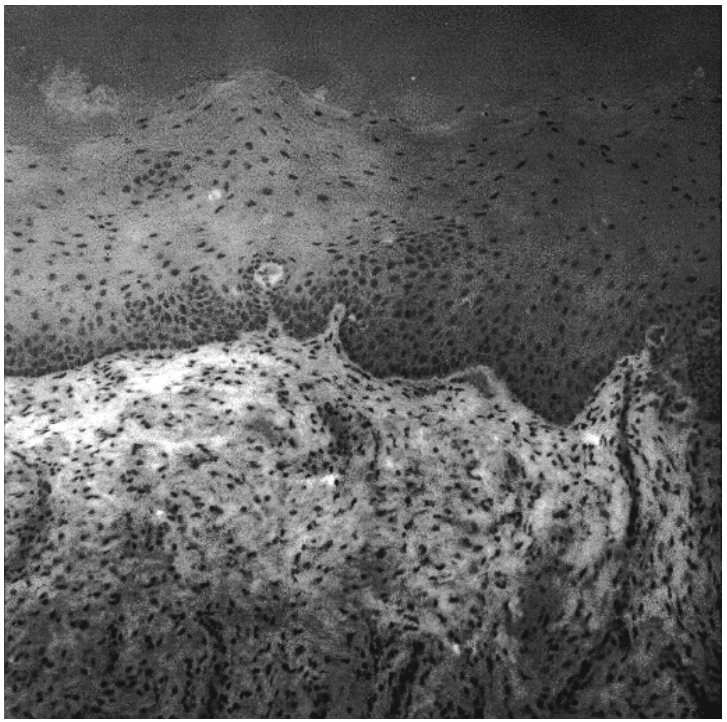

HE colored cross section of the cervix with CIN lesion

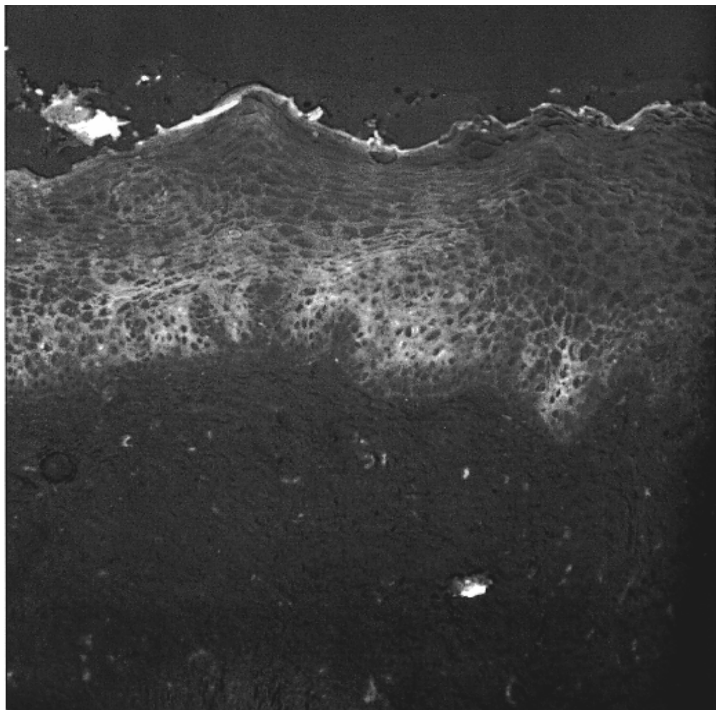

Fluorescence microscopy cross section of the cervix with low-grade CIN lesion

# Surface illumination of 30 mm long distributor (in air)

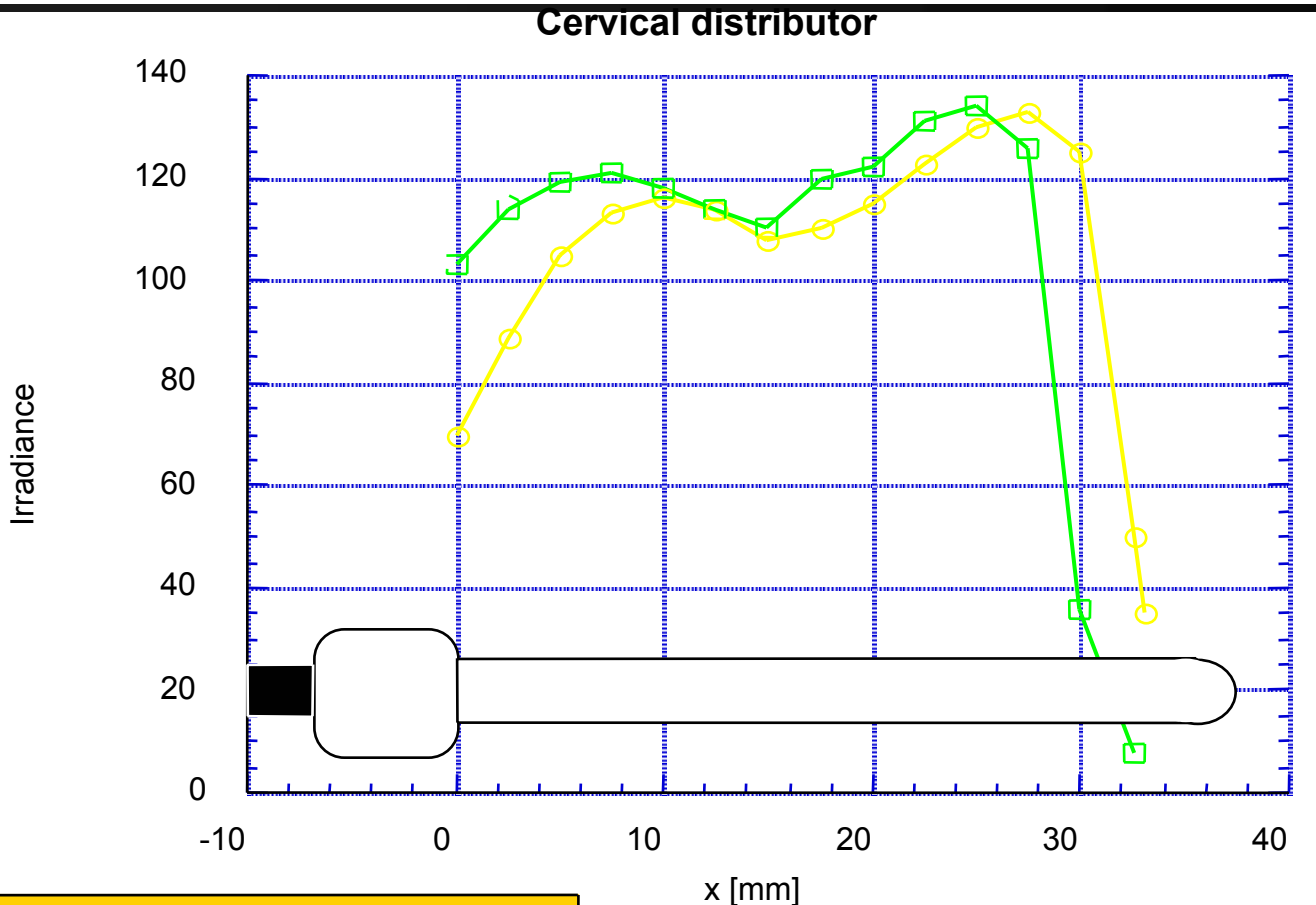


fibre in depth
fibre back at 3mm distance

# Light distributor for PDT in the cervix

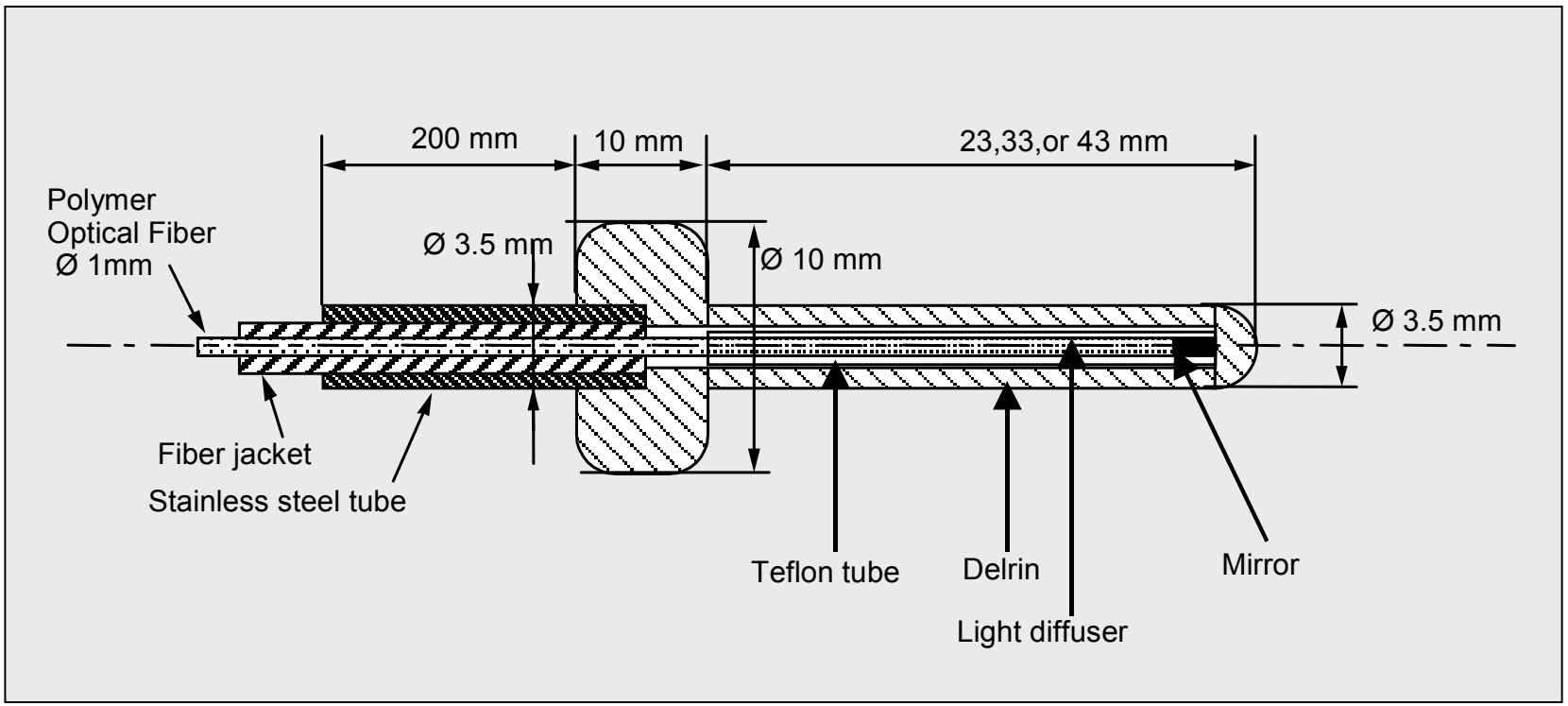

# Instrumentation set-up for the fluorescence imaging tumor depth profiling

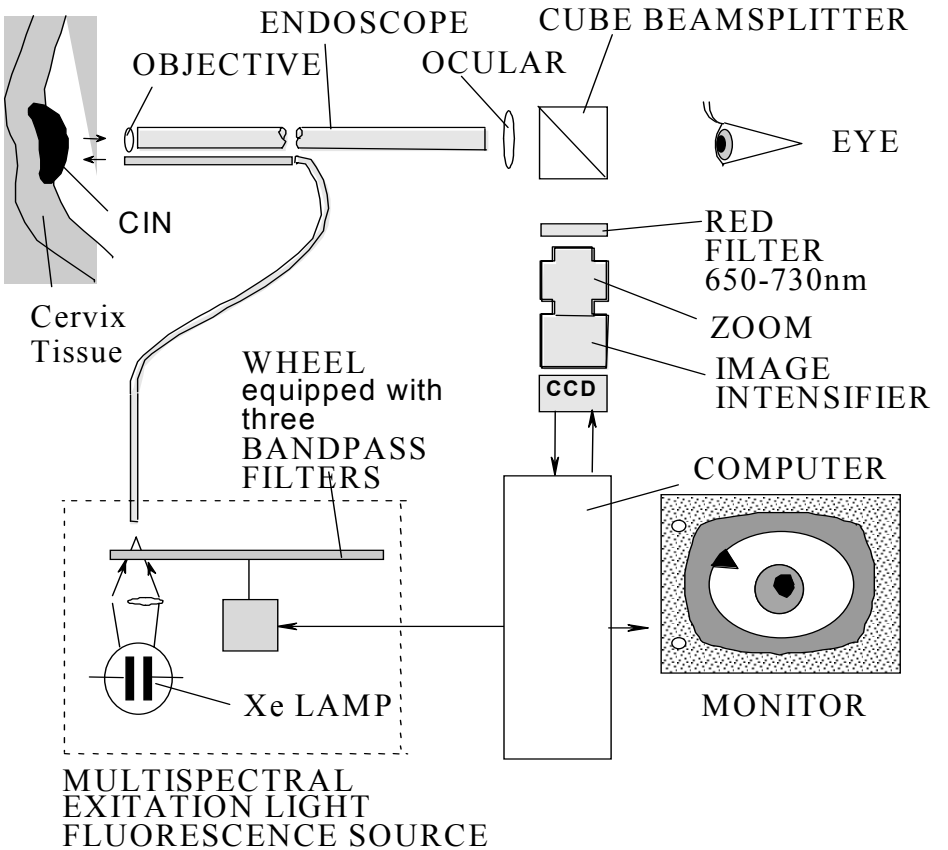

# Principle of fluorescence imaging tumor depth profiling

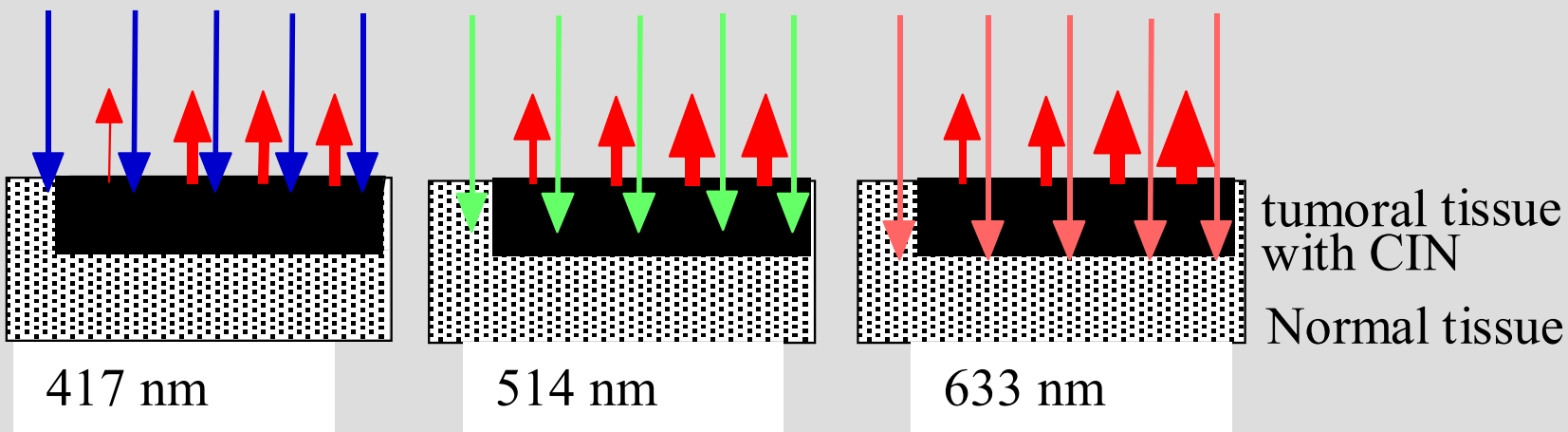


Principle of fluorescence imaging tumor depth profiling:
Homogenous exitation of the fluorochrome concentrated in the tumoral tissue at three different wavelengths, corresponding to the absorption maxima of the fluorochrome (417, 514, 633 nm)
Detection at the emission maxima (650-720) nm

# 5-Aminolevulinic acid and PPIX concentrations after oral administration (40 mg/kg b.w.). *[Rick et al. 1997]*

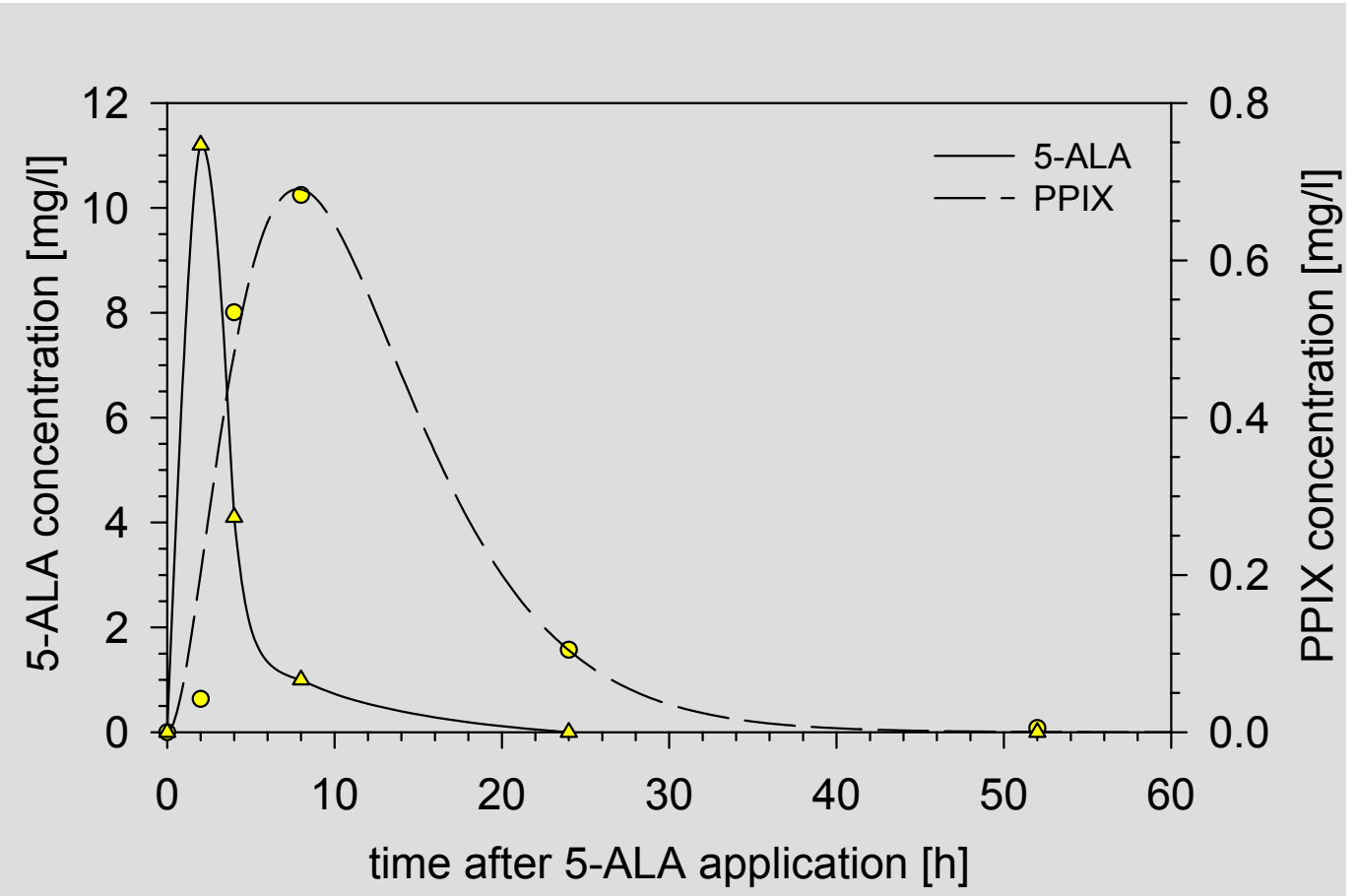

# Fluorescence intensity after oral administration of 5-aminolevulinic acid (40 mg/kg). ***[Rick et al. 1997]***